# Study of periodic solutions of the Klausmeier model


Antrea Kyprou

Supervisor: Prof. Dr. A. Doelman

MSc Mathematics

Master Thesis

June 28, 2019

Mathematical Institute, Universiteit Leiden

# Contents

# Introduction

Mathematical biology is a branch of biology which studies real life phenomena by translating them into mathematical models. Some of these phenomena describe the formation of striped patterns on zebrafish and others aggregations of reef corals. The reason of modeling of these real life phenomena is to provide an understanding of the behaviour of such systems, with the possibility of predicting future events.

A subject undergoing intense study, is vegetation patterns on sloped terrains in arid ecosystems. In environments where there is lack of rainfall, some vegetation patterns occur, in stripes or in labyrinths. These kind of vegetation were observed on aerial photographs [8], see Figure (1). Similar pictures can be found nowadays from Google Earth Satellite.

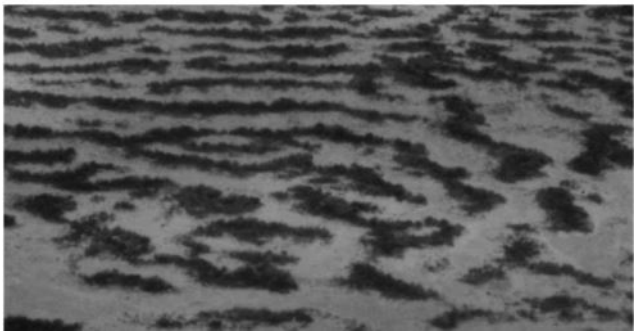

Figure 1: Striped vegetation patterns near Niamey, Niger.

This area of mathematics is quite promising since it concerns a problem about the occurrence of a "catastrophe" of some parts of the land. Catastrophe is a terminology used by ecologists when an area has become desert because of water scarcity then it's not possible to become a vegetated area again, even when there is enough rainfall. Studying and understanding the appearance

and disappearance of vegetation bands may ultimately help to prevent land degradation [14].

The intuitive reason that striped vegetation is maintained is because, while water flows in a downhill direction it reaches a vegetation stripe which absorbs the water in order to support plant growth. This water is exhausted by the downhill side of the stripe and it turns to be the next bare area. Then the stripes move uphill since the moisture level is higher towards that direction, but also because plants on the downhill side of the stripe die because of drought. In 1999, Christopher A. Klausmeier published an article [8] where he introduced a reaction-advection-diffusion system with the purpose to study the vegetation patterns in semi-arid environments. The model is a system of two partial differential equations for water component(W) and plant biomass (N) defined on a two-dimensional domain $X$ and $Y$:

$$\begin{aligned} \frac{\partial W}{\partial T} &= A - LW - RWN^2 + V\frac{\partial W}{\partial X} \\ \frac{\partial N}{\partial T} &= RJWN^2 - MN + D(\frac{\partial^2}{\partial X^2} + \frac{\partial^2}{\partial Y^2})N \end{aligned} \tag{1}$$

The parameter A is the rate of water supply, while $LW$ is the rate of water loss due to evaporation. The interesting term $RWN^2$ describes the water uptake, plants take up water at rate $RG(W)F(N)N$, where $G(W)$ is the functional response of plants to water and $F(N)$ is an increasing function which shows the water absorption by plants. For simplicity the functions $G(W)$ and $F(N)$ have been replaced with $W$ and $N$, respectively and this is how the term $RWN^2$ is formed. $V$ represents the speed at which the water flows downhill. In the next equation, $J$ describes the yield of biomass per unit water consumed and the whole term $RJWN^2$ is the plant growth. The plant biomass is lost at natural death rate of $MN$. Plant dispersal is modeled by a diffusion term with diffusion coefficient $D$.

In this thesis we will focus on the non-dimensionalized form of the model [14]:

$$\begin{aligned} \tfrac{\partial u}{\partial t} &= wu^2 - Bu + \delta^2 \Delta_{x,y}\, u \\ \tfrac{\partial w}{\partial t} &= A(1-w) - wu^2 + c\tfrac{\partial w}{\partial x} \end{aligned} \tag{2}$$

where $u$ here is the plant component. The ecological meaning of the terms doesn't change but instead of seven parameters we only have four dimensionless parameters, $A$ controls the rainfall rate, $B$ measures the plant loss, $c$ controls the rate at which water flows downhill and $\delta^2(|\delta \ll 1|)$ is the diffusion coefficient .

Our main purpose is to study the model (2) and detect where vegetation patterns occur through mathematical theory. One of the objectives is to prove the existence of homoclinic and periodic orbits. A very challenging goal of this thesis is to find the stability of these orbits. This goal is a very important aspect in this research, the stability of orbits among with parameter values can provide insights on the behaviour of pattered ecosystems.

In Chapter 1, we start by introducing a new variable $z = x - st$, which transforms the system (2) into travelling ordinary differential equations. After some rescaling and assuming that $\delta$ is a perturbation term, we find the steady states, their eigenvalues and their stability. Motivated by M. Sensi's thesis [12], we use the geometric singular perturbation theory which helps us to find where the homoclinic orbit appears. Hence, in Chapter 2 we go through the mathematical theory of Fenichel's theorem and Melnikov method [5]. We need those theorems to prove that for a specific value of the speed parameter there exists a homoclinic orbit near the desert state. The ecological interpretation of a homoclinic orbit is related to the pattern formation.

In the fourth chapter, we present another approach of the existence of a homoclinic orbit by constructing a Poincaré map. As stated above, we focus on the periodic orbits as well, consequently we find the Hopf bifurcation point and we have a range of parameter values for which periodic orbits exist. Defining the stability of these periodic orbits can help us to draw important conclusions about the pattern formation in this real life phenomenon, however the stability of the ODE solutions is not the same as in the system (2).

Thus in the last chapter, we go through the Floquet theory since this is the tool we will use to find the stability of these periodic orbits. Although, ap-

plying the Floquet theory in three dimensional equation system can become overwhelmingly complicated, therefore we include an Intermezzo section where an example of two dimensional system is set up to show the required mathematical procedure. Since the main purpose of the last chapter is to find the stability of the periodic orbits, we explain how this can be done, but without completing the necessary algebra. It is an extremely involved technical procedure but we suggest a list of steps which can be followed. Finally, we end this thesis by a short discussion section.

# Chapter 1

# Klausmeier model

As stated in the Introduction the non-dimensional form of the Klausmeier model is:

$$\begin{aligned} \frac{\partial u}{\partial t} &= wu^2 - Bu + \delta^2 \Delta_{x,y}\, u \\ \frac{\partial w}{\partial t} &= A(1-w) - wu^2 + c\frac{\partial w}{\partial x} \end{aligned} \tag{1.1}$$

and the pattern solutions of the model move in a positive direction uphill at a constant speed. This happens because the bands of vegetation which are in higher positions on the slope are the first which will absorb the water, therefore the moisture level is higher in the uphill edge. Towards the downhill direction of the slope, there is not enough water which reflects to the plant death and lower moisture levels [13]. This is the ecological explanation of pattern formation but in mathematics, migration comes from the advection term. Patterns occur after finding expressions of the travelling waves of a system. We change the variables and let $z = x - st$, $u(x,t) = U(z), w(x,t) = W(z)$, where $s$ is the migration speed. The substitution of $z$ into the model (1.1), gives the travelling wave equations:

$$\begin{aligned} \delta^2 \frac{d^2U}{dz^2} + s\frac{dU}{dz} + WU^2 - BU &= 0 \\ (c+s)\frac{dW}{dz} + A(1-W) - WU^2 &= 0 \end{aligned} \tag{1.2}$$

Moreover, water diffusivity is faster than the vegetation, therefore the system has fast and slow time scales. The best mathematical method to analyze the system is the geometric singular perturbation theory, following the paper "Geometric singular perturbation theory in biological practise" [5]. Therefore in this chapter we will start with the rescaling of the system to transform the

model into a geometric singular perturbation problem. Before studying the system through geometric singular perturbation approach, we will focus on finding the steady states of the system (1.2) and their stability since these are necessary for later on.

## 1.1 Rescaling

We introduce a new variable $P = \delta\frac{dU}{dz}$; when it's been differentiated with respect to $z$ : $\frac{dP}{dz} = \delta\frac{d^2U}{dz^2}$, the system (1.2) becomes a singular perturbation problem:

$$\begin{aligned} \frac{dU}{dz} &= \frac{P}{\delta} \\ \frac{dP}{dz} &= \frac{1}{\delta}(-\frac{sP}{\delta} + BU - WU^2) \\ \frac{dW}{dz} &= \frac{1}{(c+s)}[A(W-1) + WU^2] \end{aligned} \tag{1.3}$$

In order to remove the $\frac{1}{\delta}$ we introduce $s = \delta^2\tilde{s}$ (slow movement), so (1.3) becomes the slow system[1]:

$$\begin{aligned} \delta\frac{dU}{dz} &= P \\ \delta\frac{dP}{dz} &= -\delta\tilde{s}P + BU - WU^2 \\ \frac{dW}{dz} &= \frac{1}{(c+\delta^2\tilde{s})}[A(W-1) + WU^2] \end{aligned} \tag{1.4}$$

By rescaling the system (1.4) with the variable $\xi = z/\delta$ and using the chain rule, we get the fast form[1] of the system :

$$\begin{aligned} \frac{dU}{d\xi} &= P \\ \frac{dP}{d\xi} &= BU - WU^2 - \delta\tilde{s}P \\ \frac{dW}{d\xi} &= \frac{\delta}{(c+\delta^2\tilde{s})}[A(W-1) + WU^2] \end{aligned} \tag{1.5}$$

where $\delta$ is the perturbation parameter.

[1]These terms will be explained in detail in Chapter 2

## 1.2 Linearisation

Consider the new rescaled system (1.5), to find the steady states of the system we let $\frac{dU}{d\xi} = \frac{dP}{d\xi} = \frac{dW}{d\xi} = 0$.

- The equation $\frac{dU}{d\xi} = 0$ gives $P = 0$.
- When $P = 0$, equation $\frac{dP}{d\xi} = 0$ is $U(B - WU) = 0$, it gives $U = 0$ and $W = \frac{B}{U}$.
- When $U = 0$, equation $\frac{dW}{d\xi} = 0$ is $W - 1 = 0$ so $W = 1$.

The first steady state of the system is $(U^*, P^*, W^*) = (0, 0, 1)$.

- When $W = \frac{B}{U}$, equation $\frac{dW}{d\xi} = 0$ gives:

$$BU^2 - AU + AB = 0$$

$$U_{1,2} = \frac{A \pm \sqrt{A^2 - 4AB^2}}{2B}$$

So the other two steady states of the system are:

$$(U_+^*, P_+^*, W_+^*) = (\frac{A + \sqrt{A^2 - 4AB^2}}{2B}, 0, \frac{2B^2}{A + \sqrt{A^2 - 4AB^2}})$$

$$(U_-^*, P_-^*, W_-^*) = (\frac{A - \sqrt{A^2 - 4AB^2}}{2B}, 0, \frac{2B^2}{A - \sqrt{A^2 - 4AB^2}}).$$

In order for these steady states to be real the conditions $A, B > 0$ (the rainfall A cannot be negative) and $A \geq 4B^2$ should hold. To find the stability of the steady states we need the Jacobian matrix, but first we expand the system (1.5) with respect to $\delta^2$ and neglect terms of $\mathrm{O}(\delta^3)$, $\frac{\delta}{c+\delta^2\tilde{s}} \simeq \frac{\delta}{c}$ :

$$\begin{aligned} \frac{dU}{d\xi} &= P \\ \frac{dP}{d\xi} &= BU - WU^2 - \delta\tilde{s}P \\ \frac{dW}{d\xi} &= \frac{\delta}{c}[A(W-1) + WU^2] \end{aligned} \tag{1.6}$$

Hence the Jacobian matrix for system (1.6) is:

$$J = \begin{pmatrix} 0 & 1 & 0 \\ B - 2WU & -\delta\tilde{s} & -U^2 \\ 2\delta WU/c & 0 & \delta(A + U^2)/c \end{pmatrix}$$

Substituting the steady state $(0, 0, 1)$ in the Jacobian matrix, it becomes:

$$J = \begin{pmatrix} 0 & 1 & 0 \\ B & -\delta\tilde{s} & 0 \\ 0 & 0 & \delta A/c \end{pmatrix}$$

and the eigenvalue equation for the point (0,0,1) is :

$$\lambda^3 c + \lambda^2(-A\delta + \delta\tilde{s}c) + \lambda(-A\delta^2\tilde{s} - Bc) + AB\delta = 0 \tag{1.7}$$

By expanding $\lambda$ with the standard perturbation expansion :$\lambda \sim \lambda_0 + \delta\lambda_1 + O(\delta^2)$, the equation (1.7) becomes:

$c\lambda_0^3 + 3\delta\lambda_0^2\lambda_1 c + (\lambda_0^2 + 2\delta\lambda_1\lambda_0)(\delta\tilde{s}c - A\delta) + (\lambda_0 + \delta\lambda_1)(-A\delta^2\tilde{s} - Bc) + AB\delta = O(\delta^2)$

At the leading order we get: $c\lambda_0^3 - \lambda_0 Bc = 0$ the three eigenvalues are:

- $\lambda_{0_{(1)}} = 0$
- $\lambda_{0_{(2,3)}} = \pm\sqrt{B}$

At $O(\delta)$ the equation (1.7) is:

$$3\lambda_0^2\lambda_1 c + \lambda_0^2(\tilde{s}c - A) + \lambda_1(-Bc) + AB = 0 \tag{1.8}$$

- When $\lambda_0 = 0$, (1.8) is $\lambda_1(-Bc) + AB = 0$ so $\lambda_{1_{(1)}} = \dfrac{A}{c}$.
- When $\lambda_0 = \pm\sqrt{B}$, equation (1.8) is $3B\lambda_1 c + B(\tilde{s}c - A) + \lambda_1(-Bc) + AB = 0$, so $\lambda_{1_{(2,3)}} = -\frac{\tilde{s}}{2}$.

The eigenvalues of the steady state (0,0,1) including O($\delta$) are:

- $\lambda_1 = \dfrac{\delta A}{c}$
- $\lambda_{2,3} = \pm\sqrt{B} - \delta\frac{\tilde{s}}{2}$

We assume that $\delta$ is sufficiently small, the point (0,0,1) is a saddle point. Next, we take the steady state $(U_+^*, P_+^*, W_+^*) = (U_+^*, 0, \frac{B}{U_+^*})$ and we substitute it into the Jacobian matrix:

$$J = \begin{pmatrix} 0 & 1 & 0 \\ -B & -\delta\tilde{s} & -U_+^{*\,2} \\ 2\delta B/c & 0 & \delta(A + U_+^{*\,2})/c \end{pmatrix}$$

and the eigenvalue equation is:

$$\lambda^3 c + \lambda^2(-A\delta + \delta\tilde{s}c - \delta U_+^{*2}) + \lambda(-A\delta^2\tilde{s} + Bc - \delta^2\tilde{s}U_+^{*2}) + B\delta(U_+^{*2} - A) = 0. \tag{1.9}$$

By expanding $\lambda$ to $\lambda \sim \lambda_0 + \delta\lambda_1 + O(\delta^2)$ the characteristic equation (1.9) becomes:

$$\begin{aligned}&(\lambda_0 + \delta\lambda_1)^3 c + (\lambda_0 + \delta\lambda_1)^2(-A\delta + \delta\tilde{s}c - \delta U_+^{*2}) + \\ &(\lambda_0 + \delta\lambda_1)(-A\delta^2\tilde{s} + Bc - \delta^2\tilde{s}U_+^{*2}) + B\delta(U_+^{*2} - A) = O(\epsilon^2).\end{aligned} \tag{1.10}$$

At O(1): $c\lambda_0^3 + \lambda_0 Bc = 0$, so the eigenvalues at the leading order are:

- $\lambda_{0_{(1)}} = 0$
- $\lambda_{0_{(2,3)}} = \pm i\sqrt{B}$

At $O(\delta)$ the equation (1.9) is:

$$(3\lambda_0^2\lambda_1)c + \lambda_0^2(-A + \tilde{s}c - U_+^{*2}) + \lambda_1 Bc + B(U_+^{*2} - A) = 0. \tag{1.11}$$

- When $\lambda_0 = 0$, $\lambda_{1_{(1)}} = \frac{A - U_+^{*2}}{c}$.
- When $\lambda_0 = \pm i\sqrt{B}$, (1.11) is $-3cB\lambda_1 - B\tilde{s}c + AB + BU_+^{*2} + \lambda_1 Bc + B(U_+^{*2} - A) = 0$, so this yields to $\lambda_{1_{(2,3)}} = \dfrac{U_+^{*2}}{c} - \dfrac{\tilde{s}}{2}$.

The eigenvalues of the steady state $(U_+^*, P_+^*, W_+^*)$ including O($\delta$) are:

- $\lambda_1 = \dfrac{\delta(A - U_+^{*2})}{c}$ : *The sign of $\lambda_1$ will be explained later in Chapter 4*
- $\lambda_{2,3} = \pm i\sqrt{B} + \delta(\dfrac{U_+^{*2}}{c} - \dfrac{\tilde{s}}{2})$

In the perturbed system, steady states' stability is:

- For $\tilde{s} < \frac{2U_+^{*2}}{c}$ the equilibrium points are unstable spirals
- For $\tilde{s} > \frac{2U_+^{*2}}{c}$ they are stable spirals.

# Chapter 2

# Geometric singular perturbation theory

Since in the previous chapter we went through the rescaling of Klausmeier model to transform it into a geometric singular perturbation problem, in this chapter we will cover the geometric singular perturbation theory through Fenichel's theorems and the Melnikov method. A very helpful start for this thesis, were the first chapters of Mattia Sensi's thesis [12], where he proved the existence of a homoclinic orbit. Motivated by Mattia's work, we proved the existence of a homoclinic orbit but also the existence of periodic orbits. Before getting into that part of the thesis though, we need some mathematical background by Geertje Hek [5].

Geometric singular perturbation theory (GSPT) was introduced around 1970, with the goal of analyzing dynamical systems, mainly with biological applications. These kind of systems occur mostly in nature, thus they evolve on different time scales. GSPT is a geometric approach to problems with a clear separation in time scales [5].

## 2.1 Fenichel Theory

We consider the singularly perturbed systems of ODEs with two time scales; the first one is a system depending on a fast time scale t:

$$\begin{aligned} \dot{u} &= f(u, v, \epsilon) \\ \dot{v} &= \epsilon g(u, v, \epsilon) \end{aligned} \tag{2.1}$$

where $\dot{} = \frac{d}{dt}, u \in R^k, v \in R^l, k, l \geq 1, \epsilon$ is a small perturbation parameter $(0 < \epsilon \ll 1)$ and $f, g$ are sufficiently smooth functions.
The slow time scale is $\tau = \epsilon t$. By the chain rule, $\frac{d}{dt} = \epsilon \frac{d}{d\tau}$, system (2.1) is reformulated into:

$$\begin{array}{l} \epsilon \frac{du}{d\tau} = f(u, v, \epsilon) \\ \frac{dv}{d\tau} = g(u, v, \epsilon). \end{array} \tag{2.2}$$

Each of the scalings are naturally associated with $\lim_{\epsilon \to 0}$ of (2.1) and (2.2):

$$\begin{array}{l} \dot{u} = f(u, v, 0) \\ \dot{v} = 0 \end{array} \tag{2.3}$$

$$\begin{array}{l} 0 = f(u, v, 0) \\ \frac{dv}{d\tau} = g(u, v, 0). \end{array} \tag{2.4}$$

The latter is called the reduced system, it's a differential algebraic system and it describes the evolution of the slow variable constructed by the set $f(u, v, 0)$. Suppose there exists an $l$-dimensional manifold $\mathcal{M}_0$, containing the set $f(u, v, 0)$, we suppose that it's compact and normally hyperbolic, then by definition its eigenvalues of the Jacobian $\frac{\partial f}{\partial u}(u, v, 0)|_{\mathcal{M}_0}$ are uniformly bounded away from the imaginary axis.
Regarding the information above, Fenichel established two theorems that are useful for proving the existence of a homoclinic orbit.

**Theorem 2.1**: For $0 < \epsilon \ll 1$, there exists a manifold $\mathcal{M}_\epsilon$ that is $O(\epsilon)$ close and diffeomorphic to $\mathcal{M}_0$, and it is locally invariant under the flow of the problem (2.1).
Note: Orbits on $\mathcal{M}_\epsilon$ can leave the manifold in the slow direction, via the boundary of $\mathcal{M}_\epsilon$ and not via the directions "perpendicular" to $\mathcal{M}_\epsilon$.

**Theorem 2.2:** For $0 < \epsilon \ll 1$, there exist manifolds $\mathcal{W}^s(\mathcal{M}_\epsilon)$ and $\mathcal{W}^u(\mathcal{M}_\epsilon)$ that are $O(\epsilon)$ close and diffeomorphic to $\mathcal{W}^s(\mathcal{M}_0)$ and $\mathcal{W}^u(\mathcal{M}_0)$, respectively, and they are locally invariant under the flow of the problem (2.1).
Note: The manifolds $\mathcal{W}^s(\mathcal{M}_\epsilon)$ and $\mathcal{W}^u(\mathcal{M}_\epsilon)$ have the property that solutions in $\mathcal{W}^s(\mathcal{M}_\epsilon)$ and $\mathcal{W}^u(\mathcal{M}_\epsilon)$ decay to $\mathcal{M}_\epsilon$ at exponential rate in time in forward and backward time, respectively.

Combining the orbits from the systems (2.3) and (2.4), they may form global

structures like periodic and homoclinic orbits. A very important part of the GSPT is that it can verify the persistence of these structures which correspond to transversal intersections of stable and unstable manifolds.

## 2.2 Melnikov Method

We now consider the perturbed Hamiltonian system:

$$\begin{aligned} \dot{x} &= \frac{\partial H(x,y,v)}{\partial y} + \epsilon g_1(x,y,v) \\ \dot{y} &= -\frac{\partial H(x,y,v)}{\partial x} + \epsilon g_2(x,y,v) \\ \dot{v} &= \epsilon h(x,y,v), \end{aligned} \tag{2.5}$$

in which the variable $v \in R$ and is not periodic. In the $\epsilon = 0$ limit of the system (2.5) there exists a homoclinic orbit $\gamma^h(t; v_0)$ filled with periodic orbits in every plane $\{v = v_0\}$. Figure (2.1)(from [10]) gives the visual shape of the unperturbed flow of (2.5). A two-dimensional homoclinic manifold to a curve $\mathcal{M}_0$ is shown, which was formed by homoclinic orbits. The bounded part of the stable and unstable manifolds of $\mathcal{M}_0$, $\mathcal{W}^{s,u}(\mathcal{M}_0)$, coincide and that's why this homoclinic is part of them.

When $0 \ll \epsilon \ll 1$, the manifolds $\mathcal{W}^s(\mathcal{M}_\epsilon)$ and $\mathcal{W}^u(\mathcal{M}_\epsilon)$ do not coincide but they are $O(\epsilon)$ apart. Figure (2.2) (from [10]) represents the flow and the stable and unstable manifolds on $\mathcal{M}_\epsilon$ of the perturbed system (2.5). Furthermore, for some specific parameter values a homoclinic unperturbed orbit $\gamma^h(t; v_0)$ can survive in $\mathcal{M}_\epsilon$ and it should be a subset of $\mathcal{W}^s(\mathcal{M}_\epsilon) \cap \mathcal{W}^u(\mathcal{M}_\epsilon)$. Therefore we need to measure the distance between $\mathcal{W}^s(\mathcal{M}_\epsilon)$ and $\mathcal{W}^u(\mathcal{M}_\epsilon)$. The Melnikov method basically calculates this distance and detects whether such surviving homoclinic orbits exist.

In Figure (2.3) (from [5]), the Melnikov method can be explained better in the fixed plane $\{v = v_0\}$, for $\epsilon = 0$ and $\epsilon > 0$. It is assumed that for $\epsilon = 0$ of (2.5) a homoclinic orbit $\gamma^h(t)$ passes through a saddle point $p$ and $\gamma^h(t) = (t; v_0)$ is

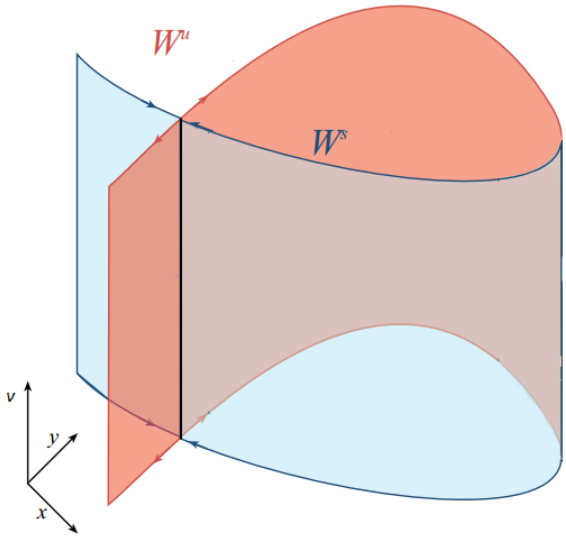


Figure 2.1: The unperturbed flow of (2.5)

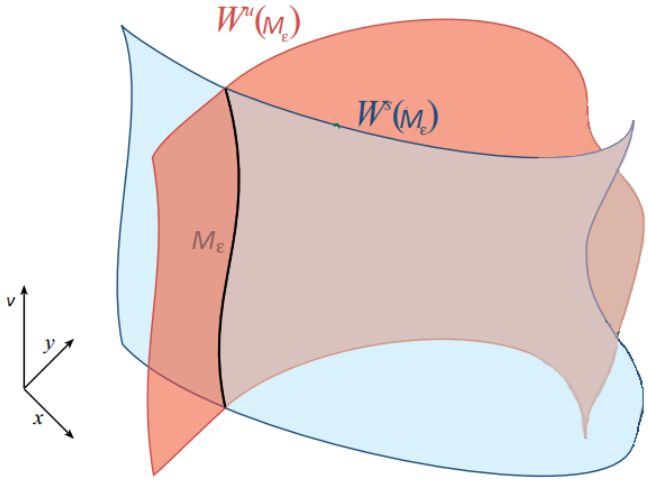


Figure 2.2: The flow of (2.5) and the perturbed stable and unstable manifolds.

the homoclinic solution in $\{v = v_0\}$ with $\gamma^h(0) = (x_0, y_0, v_0)$. $\Sigma_{v_0}$ is the line through $u_0 = (x_0, y_0)$ perpendicular to $f(\gamma^h(0; v_0))$.

Thus, if a homoclinic orbit survives then the distance between the stable and unstable manifold should be zero.

The solutions $\gamma^u_\epsilon$ in $\mathcal{W}^u(\mathcal{M}_\epsilon)$ and $\gamma^s_\epsilon$ in $\mathcal{W}^s(\mathcal{M}_\epsilon)$ to perturbed system (2.5) are determined by the initial condition $\gamma^{u,s}_\epsilon(0) \in \Sigma_{v_0}$.

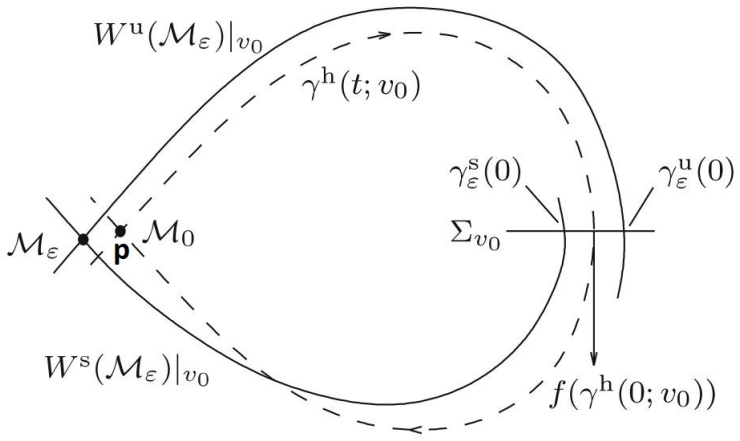


Figure 2.3: Melnikov method in the plane $\{v = v_0\}$

Then the distance between the stable and the unstable manifolds can be expressed as the dot product of the difference between $\gamma^s_\epsilon$ and $\gamma^u_\epsilon$ with the perpendicular vector filed $f \perp (\gamma^h(0;v_0) = (\frac{\partial H}{\partial x}(\gamma^h(0;v_0)), \frac{\partial H}{\partial y}(\gamma^h(0;v_0)))^T$:

$$\Delta(t=0,v_0,\epsilon) = f(\gamma^h(0;v_0)) \wedge [\gamma^u_\epsilon((0;v_0) - \gamma^s_\epsilon((0;v_0)], \tag{2.6}$$

where $\wedge$ is called wedge product and it's defined by $a \wedge b = a_1b_2 - a_2b_1$ and $f \wedge [\gamma^u_\epsilon - \gamma^s_\epsilon]$ is the projection of $\gamma^y_\epsilon - \gamma^s_\epsilon$ on the perpendiculat vector field $f$. However, $\Delta_\epsilon$ depends on section $\Sigma_{v_0}$, so if we reformulate (2.6) then the expression on finding the distance between the two manifolds won't be affected by $\Sigma_{v_0}$:

$$\Delta(0,v_0) = \frac{\partial}{\partial\epsilon}\Delta(t=0,v_0,\epsilon)|_{\epsilon=0} = f(\gamma^h(0;v_0)) \wedge [\frac{\partial}{\partial\epsilon}\gamma^u_\epsilon(0;v_0) - \frac{\partial}{\partial\epsilon}\gamma^s_\epsilon(0;v_0)], \tag{2.7}$$

which measures the distance between the manifolds in the plane $\{v = v_0\}$ at $\mathrm{O}(\epsilon)$,(see [5] for details) :

$$\Delta W(v_0) = \int_{-\infty}^{\infty} f(\gamma^h(0;v_0)) \wedge \left[ g(\gamma^u_\epsilon(0;v_0)) + \frac{\partial f}{\partial v}(\gamma^u_\epsilon(0;v_0))\frac{\partial v}{\partial \epsilon}\right] dt \tag{2.8}$$

where $\frac{\partial v}{\partial \epsilon}$ satisfies $\frac{d}{dt}(\frac{\partial v}{\partial \epsilon}) = h(\gamma^h(0;v_0))$ and $\frac{\partial v}{\partial \epsilon} = 0$ at t=0, $\Delta W(v_0) = 0$ means that $\mathcal{W}^s(M_\epsilon)$ and $\mathcal{W}^u(M_\epsilon)$ have transverse intersection and hence survival of the original homoclinic orbit. Moreover, although if the integral (2.8) uses

perturbed ($\epsilon \neq 0$) equations to find the distance of the manifolds in the perturbed flow of the system, the integration is along solutions of the unperturbed system.

The Melnikov method (2.8) can be applied to more general systems, however we will use the integral of the derivative Hamiltonian H, which is not constant of the motion in the perturbed system. According to the literature [5] in case of a Hamiltonian system (2.5), for $\epsilon > 0$ a connecting orbit $\gamma^h(t)$ to $\mathcal{M}_\epsilon$ must satisfy $\lim_{t\to\infty} H(\gamma^h(t)) = \lim_{t\to-\infty} H(\gamma^h(t))$ and if H is constant on $\mathcal{M}_0$, then $\Delta H|_{\gamma^h} = \int_{-\infty}^{\infty} \frac{dH}{dt}(\gamma^h(t))dt = 0$ must hold. $\Delta H$ describes the distance between $\mathcal{W}^s_\epsilon(M_0)$ and $\mathcal{W}^u\epsilon(M_0)$.

# Chapter 3

# Homoclinic orbit

This chapter is about applying the mathematical theory of Chapter 2 to the Klausmeier model in order to show the existence of a homoclinic orbit. According to the geometric singular perturbation theory, the example systems (2.1) and (2.2) of Chapter 2 are related to the ODE systems (1.5) and (1.4) representing the fast and the slow systems respectively.
Hence, following the theory in Chapter 2 and an application example of Fenichel's Theorem 2.2 [5], we will focus on the perturbed ODE system (1.5). Taking the $\lim_{\delta \to 0}$ of (1.5) yields:

$$\begin{aligned} \frac{dU}{d\xi} &= P \\ \frac{dP}{d\xi} &= BU - WU^2 \\ \frac{dW}{d\xi} &= 0 \end{aligned} \tag{3.1}$$

which is the unperturbed system. Referring back to the first chapter, the steady states are $\tilde{S} = (0, 0, 1)$ and $C^{\pm} = (\frac{A \pm \sqrt{A^2 - 4AB^2}}{2B}, 0, \frac{2B^2}{A \pm \sqrt{A^2 - 4AB^2}})$. The biological meaning of the saddle point $\tilde{S}$ is defined as a desert state because the vegetation component is zero.
For $\delta = 0$, the system (3.1) has two manifolds of equilibria. The normally hyperbolic is $\mathcal{M}_0 = \{U = P = 0, W = W_0\}$ and the non-hyperbolic is $\mathcal{N}_0 = \{U = B/W, P = 0, W = W_0\}$.

According to Fenichel's Theorem 2.1, for sufficiently small $\delta$, there exists a manifold $\mathcal{M}_\delta$ that is $O(\delta)$ close and diffeomorphic to $\mathcal{M}_0$ under the invariant flow of (1.5). Going back to Chapter 1, the eigenvalues when $\delta = 0$

are: $\lambda = 0, \pm\sqrt{B}$, which correspond to the invariant manifold, and the 2-dimensional stable ($W^s(\mathcal{M}_0)$) and unstable ($W^u(\mathcal{M}_0)$) manifolds, respectively. Bringing the model (1.1) into a simpler form of (1.5), gives us the option to study the global behaviour of $W^s(\mathcal{M}_0)$ and $W^u(\mathcal{M}_0)$ in the plane $\{W = W_0\}$. The 3-D phase portrait of this case is displayed in Figure (3.1).

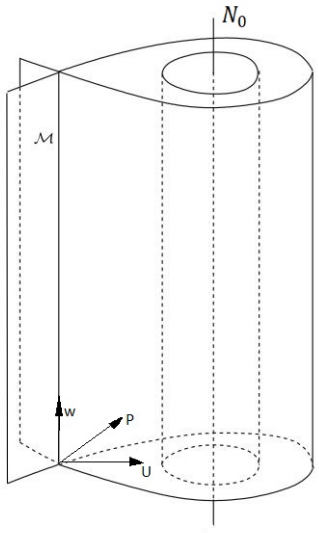


Figure 3.1: This phase portrait of $\delta = 0$, shows the normally hyperbolic $\mathcal{M}_0$ and non-hyperbolic $\mathcal{N}_0$ manifolds, where the saddle point $\tilde{S} = (0, 0, 1)$ lies on $\mathcal{M}_0$ and the points $C^{\pm} = (U^*, 0, B/U^*)$ lie on $\mathcal{N}_0$.

By using the Theorem 2.2, $W^s(\mathcal{M}_0)$ and $W^u(\mathcal{M}_0)$ persist as perturbed manifolds $W^s(\mathcal{M}_\delta)$ and $W^u(\mathcal{M}_\delta)$, that are $\mathrm{O}(\delta)$ close and diffeomorphic to $W^s(\mathcal{M}_0)$ and $W^u(\mathcal{M}_0)$ under the invariant flow of (1.5). The phase portrait of the perturbed system is shown in Figure (3.2).

Since the manifold $\mathcal{M}_0$ is still invariant in the perturbed system (1.5), we can choose that $\mathcal{M}_0 = \mathcal{M}_\delta$, in order to prove that a homoclinic orbit survives the perturbation, we need to tune the speed parameter $\tilde{s}$. Hence, we have to show that for a unique value of $\tilde{s} = \tilde{s}^*$ and a sufficiently small $\delta$, the system has a connecting homoclinic orbit to the saddle point $\tilde{S}$.
For any value of $\tilde{s}$, $W^u_\delta(\mathcal{M}_0) \cap W^s_\delta(\mathcal{M}_0) = W^u_\delta(\tilde{S}) \cap W^s_\delta(\mathcal{M}_0)$, because the W-axis is unstable with respect to $\tilde{S}$ and any point on $W^u_\delta(\mathcal{M}_0)$ will tend to $\tilde{S}$ as $\xi \to -\infty$ [12].

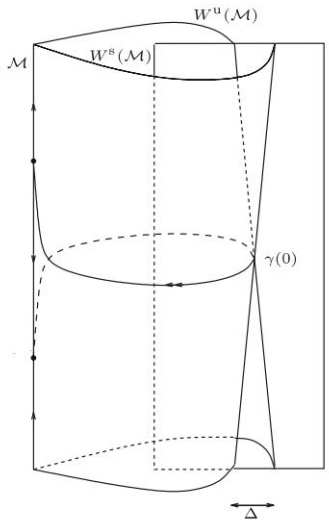


Figure 3.2: Phase portrait of the perturbed system (1.5)

In order to prove the existence of a homoclinic orbit we need to point out some geometrical arguments from Figures (3.2) and (3.3). The three cases in Figure (3.3) of different values of the parameter $\tilde{s}$ are presented on $u = 0$, $\mathcal{W}^s$ and $\mathcal{W}^u$ are the curves generated by the first intersection of $W^s_\delta(\mathcal{M}_0)$ and $W^u_\delta(\mathcal{M}_0)$ (also shown in Figure (3.2)), respectively, with $u = 0$. $\gamma(0)$ is the intersection of $\mathcal{W}^s$ and $\mathcal{W}^u$ close to a $W_0$ point on the W-axis and X is the point where the stable manifold of $W_0$ intersects with $\mathcal{W}^s$, as $\xi \to \infty$ a homoclinic orbit starting from a point in the W-axis has to pass through X.
In Figure (3.3) we can see what happens when $\tilde{s} < \tilde{s}^*$ , $\tilde{s} = \tilde{s}^*$ and $\tilde{s} > \tilde{s}^*$. When $\tilde{s} < \tilde{s}^*$, the unstable manifold of $W_0$ moves away from the W-axis, it reaches $\gamma(0)$ and then it goes back to the W-axis but not back where it started. Although when $\tilde{s} > \tilde{s}^*$, a point($W_0$) starting from W-axis follows the unstable manifold of $\mathcal{M}_\epsilon$, it reaches the intersection of $\mathcal{W}^s$ and $\mathcal{W}^u$ and then it follows the stable manifold and returns close in $\delta$ to the W-axis but it's repulsed slowly away from it.
But when $\tilde{s} = \tilde{s}^*$ a homoclinic orbit survives, the unstable manifold of the point $W_0$ reaches the intersection of $\mathcal{W}^s$ and $\mathcal{W}^u$ and then it returns back to the initial point, assuming that the point $W_0$ is the saddle point $\tilde{S}$ then $W^u_\delta(\tilde{S}) \cap W^s_\delta(\mathcal{M}_0) = W^u_\delta(\tilde{S}) \cap W^s_\delta(\tilde{S}) = \gamma^{hom}_\delta(\xi)$.

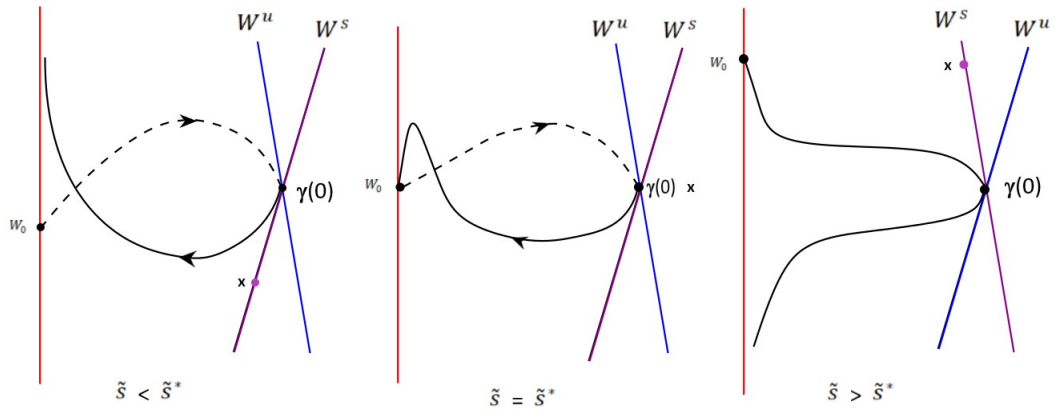


Figure 3.3: The three cases for $\tilde{s}$ on $u = 0$, the vertical direction is the W-axis

In order to find the value of $\tilde{s}^*$ where the homoclinic orbit exists, we start by finding the Hamiltonian equation from the fast system (3.1) where $W = W_0$:

$$\frac{dU}{d\xi} = \frac{dH}{dP}, \qquad \frac{dP}{d\xi} = -\frac{dH}{dU}$$

Solving $\frac{dH}{dP} = P$ by separation of variables: $H(U,P) = \frac{P^2}{2} + K(U)$ and $\frac{dH}{dU} = W_0U^2 - BU$: $H(U,P) = \frac{W_0U^3}{3} - \frac{BU^2}{2} + E(P)$ where $K(U)$ and $E(P)$ are arbitary functions. Therefore the Hamiltonian is :

$$H(U,P) = \frac{P^2}{2} + \frac{W_0U^3}{3} - \frac{BU^2}{2} \tag{3.2}$$

The (1.5) has a family of homoclinic orbit solutions (see [5] (3.4)) :

$$U_0 = \frac{3B}{2W_0}\operatorname{sech}^2(\frac{1}{2}\sqrt{B}\xi), \qquad P_0 = \frac{d}{d\xi}U_0(\xi), \tag{3.3}$$

these form a homoclinic orbit to the point $(0, 0, W_0)$, however in the perturbed system the only value of $W_0$ for which we have an equilibrium point in the W-axis is at W=1. However, no conclusion can be drawn about the intersection of $W^s(\mathcal{M}_\delta)$ and $W^u(\mathcal{M}_\delta)$ through Fenichel's theorems. Thus we need to apply Melnikov method.

## 3.1 Application of Melnikov Method

The last point of Chapter 2 ($\Delta H|_{\gamma^h} = \int_{-\infty}^{\infty} \frac{dH}{dt}(\gamma^h(t))dt = 0$) is the key to our aim. Consequently, we need to find the differentiation of the Hamiltoninan with respect to $\xi$, in the perturbed system.

$$\begin{aligned} H_\xi &= PP_\xi - BUU_\xi + W_0U^2U_\xi + \tfrac{U^3W_\xi}{3} \\ &= \delta[-\tilde{s}P^2 + \tfrac{U^3}{3c}(A(W_0-1) + W_0U^2)] \end{aligned} \tag{3.4}$$

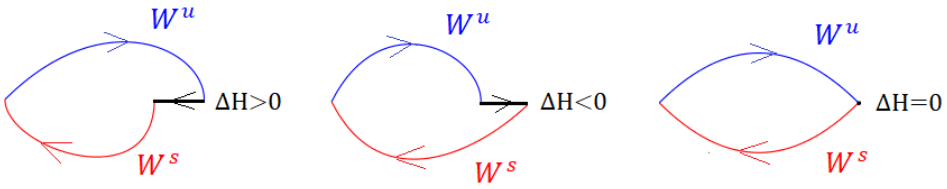


Figure 3.4: Distance between the stable and unstable manifolds

The next step is to separate the Hamiltonian to fast and slow flow, according to Chapter 2 and Fenichel's theorem, $H(U,P)$ is the fast flow and as $\xi \to \infty$ the solutions (3.3) $(U_0(\xi), P_0(\xi)) \to (0,0)$.
As mentioned in the Section 2.2, the integration in Melnikov method is along solutions of the unperturbed system even if the integral uses perturbed equations, therefore we will compute $\Delta H$ along $(U_0(\xi), P_0(\xi), W_0)$.
By rewriting the Hamiltonian (3.4) in the form of: $\frac{dH}{d\xi} = \delta[F(U_0(\xi), P_0(\xi), W_0) + \delta G(W_0)]$:

$$\Delta H(W_0) = \delta \int_{-\infty}^{+\infty} [F(U_0(\xi), P_0(\xi), W_0) + \delta G(W_0)]d\xi$$

$$= \delta \int_{-\infty}^{+\infty} F(U_0(\xi), P_0(\xi), W_0)d\xi + \delta^2 \int_{-\infty}^{+\infty} G(W_0)d\xi = \infty$$

However as we see in Figure (3.4), the homoclinic orbit exists when $\Delta H = 0$, the orbits on $\mathcal{W}^s(\mathcal{M}_0) \cap \mathcal{W}^u(\mathcal{M}_0)$ are exponentially close to $\mathcal{M}_0$ at the boundary, so we can change the limits to $\pm\frac{1}{\sqrt{\delta}}$:

$$\Delta H(W_0) = \delta \int_{-\frac{1}{\sqrt{\delta}}}^{\frac{1}{\sqrt{\delta}}} F(U_0(\xi), P_0(\xi), W_0)d\xi + \delta^2 \int_{-\frac{1}{\sqrt{\delta}}}^{\frac{1}{\sqrt{\delta}}} G(W_0)d\xi$$

Substituting the solutions of family of homoclinic orbits (3.3) into the integral above and changing the boundaries to $\pm\infty$ as $F(U_0(\xi), P_0(\xi), W_0)$ converges to 0 as $\xi \to \pm\infty$:

$$\Delta H(W_0) = \delta \int_{-\infty}^{+\infty} F(U_0(\xi), P_0(\xi), W_0) d\xi + O(\delta^{\frac{3}{2}})$$

And now we use the condition $\Delta H|_{\gamma^h} = \int_{-\infty}^{\infty} \frac{dH}{dt}(\gamma^h(t))dt = 0$:

$$\begin{aligned} \Delta H(W_0, \tilde{s}) &= \int_{-\infty}^{+\infty} \frac{dH}{d\xi} d\xi + O(\delta) \\ &= \delta \int_{-\infty}^{+\infty} -\tilde{s}P_0^2 + \frac{U_0^3}{3c}(A(W_0 - 1) + W_0 U_0^2) d\xi + O(\delta^2) \end{aligned}$$

To calculate this integral way easier, we only consider $W_0 = 1$, since we are specifically looking for the existence of a homoclinic orbit at the saddle point $\tilde{S} = (0, 0, 1)$.

$$\begin{aligned} \Delta H(1, \tilde{s}) &= \delta \int_{-\infty}^{\infty} -\tilde{s}P_0^2 + \frac{U_0^5}{3c} d\xi \\ &= \delta \int_{-\infty}^{\infty} -\tilde{s}\frac{9B^3}{4} \operatorname{sech}^4(\tfrac{\sqrt{B}\xi}{2}) \tanh^2(\tfrac{\sqrt{B}\xi}{2}) + \frac{243B^5}{96c} \operatorname{sech}^{10}(\tfrac{\sqrt{B}\xi}{2}) d\xi \end{aligned} \tag{3.5}$$

Now

$$\begin{aligned} &\int_{-\infty}^{\infty} \operatorname{sech}^4(\frac{\sqrt{B}\xi}{2}) \tanh^2(\frac{\sqrt{B}\xi}{2}) d\xi \\ &= \left[ \frac{2(\cosh(\sqrt{B}\xi) + 4) \tanh^3(\frac{\sqrt{B}\xi}{2}) \operatorname{sech}^2(\frac{\sqrt{B}\xi}{2})}{15\sqrt{B}} \right]_{-\infty}^{\infty} \\ &= \frac{8}{15\sqrt{B}} \end{aligned} \tag{3.6}$$

and

$$\int_{-\infty}^{\infty} \operatorname{sech}^{10}(\frac{\sqrt{B}\xi}{2})d\xi = \frac{2}{315\sqrt{B}}\Big[130\cosh(\sqrt{B}\xi) + 46\cosh(2\sqrt{B}\xi) + 10\cosh(3\sqrt{B}\xi)$$

$$+ \cosh(4\sqrt{B}\xi) + 128)\tanh(\tfrac{\sqrt{B}\xi}{2})\operatorname{sech}^{8}(\tfrac{\sqrt{B}\xi}{2})\Big]_{-\infty}^{\infty}$$

$$= \frac{512}{315\sqrt{B}} \tag{3.7}$$

Thus $\Delta H = 0$:

$$\frac{8}{15\sqrt{B}} \times \frac{9B^3}{4}\tilde{s} = \frac{512}{315\sqrt{B}} \times \frac{243B^5}{96c}$$

$$\tilde{s} = \tilde{s}^* = \frac{24B^2}{7c} \tag{3.8}$$

Therefore, for $s = \delta^2\tilde{s}$, where $\tilde{s}^* = \dfrac{24B^2}{7c}$, there exists a homoclinic orbit to the saddle point $\tilde{S}$ for the system (1.5).

# Chapter 4

# Poincaré map

Another way to prove the existence of a homoclinic orbit which passes through the saddle point $\bar{S} = (0, 0, 1)$ is by constructing a Poincaré map since it preserves many properties of periodic and quasiperiodic orbits. An approximation of a Poincaré map can determine the existence but also the stability of periodic orbits. However, in this chapter we will focus only on the existence of homoclinic and periodic orbits.

## 4.1 Definition

A **Poincaré map** is also known as a first return map, it's a type of map that is helpful analyzing a system that appears to have periodic behaviour.
A map is defined by a function $P : M \to M$ through the relation $x' = P(x)$, where $x' \in M$ denotes the new point that arises from the initial point $x \in M$. For a map, an orbit is no longer a function $x(t)$ of $t \in R$ but is instead a sequence $\{x_t : t \in Z\}$. Using this subscript notation, the dynamics is given by the iteration $x_t = P(x_{t-1})$.
Maps arise naturally from flows by taking sections of the flow. For a flow in $R^n$, a section, S, is a surface of dimension $d = n - 1$ such that the velocity vector is not tangent to S at any point. That is, if $\hat{n}_x$ is the unit normal to S at $x$, then S is a section if $f(x) \cdot \hat{n}_x \neq 0$ for all $x \in S$.
A Poincaré map for a section S is obtained by choosing an $x \in S$, and following the flow $\phi_t(x)$ to find the first return to S: let $\tau(x)$ be the first positive time for which $\phi_t(x) \in S$. The map is defined by $P(x) = \phi_{\tau(x)}(x)$ [10].
If a point maps to itself, it means that the point is a fixed point of the map

and it's a limit cycle on the original flow.

## 4.2 Construction of a Poincaré map

Consider the 3D ODE system (1.6). The periodic orbits of this perturbed system must be $O(\delta)$ close to some periodic orbits of the unpertrubed system:

$$\begin{aligned} \frac{dU}{d\xi} &= P \\ \frac{dP}{d\xi} &= BU - WU^2 \\ \frac{dW}{d\xi} &= 0. \end{aligned} \tag{4.1}$$

Recall from the previous chapter that the Hamiltonian equation of the system (4.1) is:

$$H(U,P) = \frac{P^2}{2} + \frac{W_0U^3}{3} - \frac{BU^2}{2} \tag{4.2}$$

When the steady states of the system (1.6) are substituted into (4.2) we can see that:

- the saddle point $\bar{S} = (0,0)$ corresponds to $H = H_s = 0$ and
- the center points $C^{\pm} = (B/W_0, 0)$ correspond to $H = H_c = \frac{-B^3}{6W_0^2}$

From Figure (3.1), for $H \in (H_c, H_s)$, system (4.1) has periodic solutions. For any value of $H > 0$ the solutions are unbounded. The periodic orbits to (4.1) can be uniquely described by a pair (H,W). This map is only defined for $H$ in an $O(\delta)$ neighborhood of $H \in (-\frac{B^3}{6W_0^2}, 0)$, as shown in Figure (4.1), for the full perturbed system (1.5).

Any return point of the Poincaré map is defined as $P(H,W)$, if this point returns to where it was at first, then $P(H,W) = (H,W)$; it is a fixed point on the Poincaré map, which means is a periodic orbit in the original flow of the dynamical system. The approximation of the Poincaré map is [4, 2, 1] :

$$P(H,W) = (H + \delta\Delta W(H,W), W + \delta\Delta W(H,W)) \tag{4.3}$$

where $\Delta W(H_0,W_0)$ and $\Delta H(H_0,W_0)$ measure the accumulated change in the slow variable H and W of a solution (1.6).

$$\Delta W(H_0,W_0) = \int_0^{T_\delta(H_0,W_0)} W_\xi(U_\delta, P_\delta, W_\delta)d\xi \tag{4.4}$$

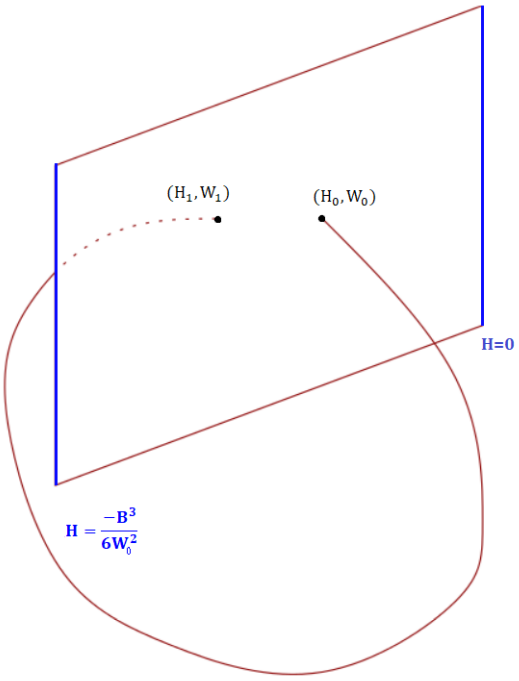


Figure 4.1: Poincaré map

$(U_\delta, P_\delta, W_\delta)$ is the flow of the system (1.6) and $T_\delta(H_0, W_0)$ is the return time. Rearranging the Hamiltonian equation we get:

$$P^2 = 2H - \frac{2W_0U^3}{3} + BU^2$$

Let $P^2 = G_H(U)$ so $P(U) = \pm\sqrt{G_H(U)}$.

Figure (4.2) shows the phase portrait of the system (4.1) in 2 dimensions to make the demonstration of the system easier. It represents the three cases of $H = 0, H = -\frac{B^3}{6W_0}$ and $H > 0$, the two steady states and a periodic orbit enclosed by the homoclinic orbit when H=0.
Further, we focus on the periodic orbit of (4.1) near the center point $(\frac{B}{W_0}, 0)$. This periodic orbit can be defined as a solution $(U_0(\xi), P_0(\xi), W_0)$ of (4.1) as used in chapter three. The positive part of the periodic orbit has the expression of $P(U) = \sqrt{G_H(U)}$ and the negative one is $P(U) = -\sqrt{G_H(U)}$.
The next step is to find the values of $U$, where the periodic orbit intersects with the U-axis, therefore $P = 0$.
When H=0, $U^2(\frac{W_0U}{3} - \frac{B}{2}) = 0$, the intersection points are:

- U=0, double root and
- $U = \frac{3B}{2W_0}$

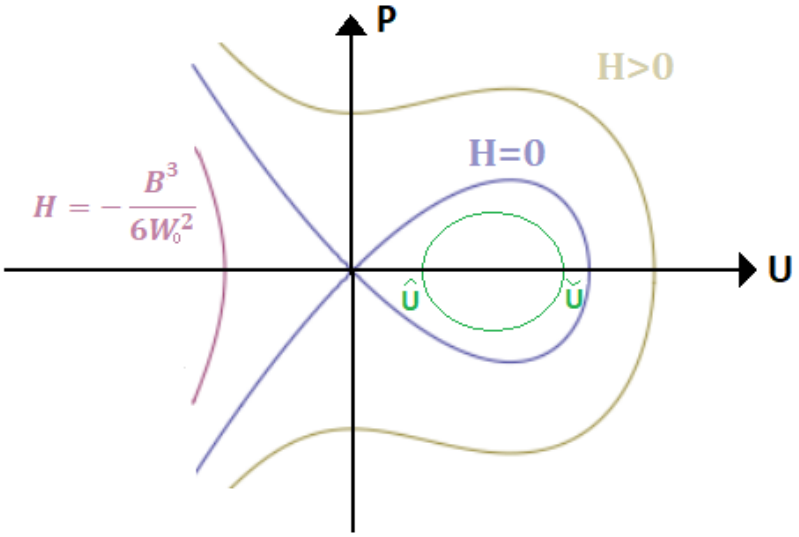


Figure 4.2: The three cases of hamiltonian

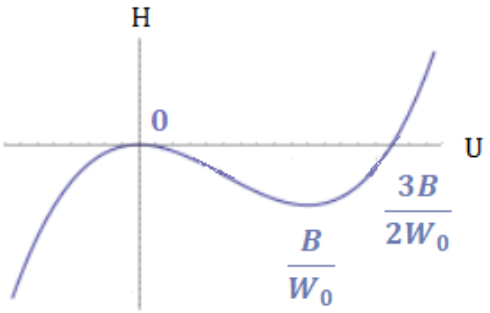


Figure 4.3: Intersection points of the orbit when H=0, P=0

From figure (4.3), we can conclude that the limits of the periodic orbit can exist only when:

$$0 < \hat{U} < \frac{B}{W_0} < \check{U} < \frac{3B}{2W_0}.$$

Going back to the equation (4.4) and the system (1.6), (4.4) can be written as:

$$\Delta W(H_0, W_0) = \frac{\delta}{c}\int_0^{T_0(H_0)} [A(W_0 - 1) + W_0 U_0(\xi)^2] d\xi + O(\delta^2)$$

where $T_0(H_0)$ is the period of the unperturbed periodic solution. Using all the information above, and changing the varibles since the limits are in terms of U, we get: $\frac{dU}{d\xi} = \frac{dH}{dP}$ , $\frac{dH}{dP} = P$ therefore $\frac{dU}{d\xi} = P$, $d\xi = \frac{dU}{P}$.

$$\Delta W(H_0, W_0) = \frac{\delta}{c}\int_{\hat{U}}^{\check{U}} \frac{A(W_0 - 1) + W_0 U_0^2}{\sqrt{G_H(U)}} dU + \frac{\delta}{c}\int_{\check{U}}^{\hat{U}} \frac{A(W_0 - 1) + W_0 U_0^2}{-\sqrt{G_H(U)}} dU \tag{4.5}$$

The integral $\int_{\check{U}}^{\hat{U}} \frac{A(W_0-1)+W_0U_0^2}{-\sqrt{G_H(U)}} dU$ needs change of limits to be mathematically correct. $\hat{U}$ has to be the lower limit and $\check{U}$ the upper one:

$$\Delta W(H_0, W_0) = \frac{2\delta}{c}\int_{\hat{U}}^{\check{U}} \frac{A(W_0 - 1) + W_0 U_0^2}{\sqrt{G_H(U)}} dU + O(\delta^2)$$

Introducing [4]

$$T_i(H) = \oint \frac{U^i}{\sqrt{G_H(U)}} dU \tag{4.6}$$

then

$$\Delta W(H, W)/2\delta = \frac{1}{c}[A(W - 1)T_0(H) + WT_2(H)] + O(\delta). \tag{4.7}$$

Similarly for $\Delta H$:

$$\Delta H(H_0, W_0) = \int_0^{T_\delta(H_0, W_0)} H_\xi(U_\delta, P_\delta, W_\delta) d\xi.$$

We differentiate the Hamiltonian equation with respect to $\xi$, in the perturbed system:

$$H = \frac{P^2}{2} + \frac{WU^3}{3} - \frac{BU^2}{2}$$

$$\frac{dH}{d\xi} = PP_\xi + U^2 WU_\xi + \frac{U^3}{3}W_\xi - BUU_\xi \tag{4.8}$$

$$H_\xi = \delta(-\tilde{s}P^2 + \frac{U^3}{3c}(A(W_0 - 1) + W_0 U^2))$$

Then,

$$\Delta H(H_0, W_0) = \delta \int_{\hat{U}}^{\check{U}} [-\frac{\tilde{s}P^2}{P} + \frac{U^3}{3Pc}(A(W_0 - 1) + W_0 U^2)] dU +$$

$$\delta \int_{\check{U}}^{\hat{U}} \delta[-\frac{\tilde{s}P^2}{P} + \frac{U^3}{-3Pc}(A(W_0 - 1) + W_0 U^2)] dU$$

$$\Delta H(H_0, W_0) = 2\delta \int_{\hat{U}}^{\check{U}} -\tilde{s}\sqrt{G_H(U)} + \frac{U^3(A(W_0-1)+W_0U^2)}{3c\sqrt{G_H(U)}}dU$$

Introduce [4],

$$S_i(H) = \oint U^i \sqrt{G_H(U)}dU \tag{4.9}$$

$$\Delta H(H, W)/2\delta = -\tilde{s}S_0(H) + \frac{A(W-1)T_3(H)}{3c} + \frac{WT_5(H)}{3c} + O(\delta) \tag{4.10}$$

$\Delta H(H, W) = \Delta W(H, W) = 0$ determines the location of periodic solutions to the system (1.6). For any fixed pair of $(H, W)$ there exists a unique pair $(A_0(H_0, W_0), \tilde{s_0}(H_0, W_0))$ (rainfall, speed). Equating the equations (4.7) and (4.10) to 0 yields a linear $(2 \times 2)$ system in the unknowns $(A, \tilde{s})$:

$$\begin{pmatrix} \frac{(W-1)T_0(H)}{c} & 0 \\ \frac{(W-1)T_3(H)}{3c} & -S_0(H) \end{pmatrix} \begin{pmatrix} A \\ \tilde{s} \end{pmatrix} = \begin{pmatrix} 0 \\ 0 \end{pmatrix} \tag{4.11}$$

Thus for a given $(H_0, W_0)$, we can derive conditions from the system (4.11) on $(A, \tilde{s})$.

The limit of this unique pair $(A_0(H_0, W_0), \tilde{s_0}(H_0, W_0))$ as $H \uparrow H_s = 0$, derives the explicit expression for the curve of global bifurcation.

$$C_{glob} = \{(A^*(W), \tilde{s^*}(W))\} = \{(\lim_{H\uparrow H_s} A_0(H, W), \lim_{H\uparrow H_s} \tilde{s_0}(H, W)\},$$

$C_{glob}$ defines a boundary in the $A - \tilde{s}$ parameter-plane, of the region $P$ in which system (1.6) has periodic solutions. Homoclinic Bifurcation occur when a periodic orbit collides with a homoclinic orbit (for period $T_0 \uparrow \infty$), and it causes changes of the trajectories in the phase space. Our aim is to derive a condition of the parameters of $(A^*(W), \tilde{s^*}(W))$ to find where the homoclinic bifurcation occurs.

In order to find the global bifurcation point, we need to make some modification to $\Delta H$ and $\Delta W$ for algebraic simplicity. First, we will start by writing $S_i$ in terms of $T_{i+k}$:

$$S_i = \oint \frac{U^i G_H}{\sqrt{G_H}}dU = \oint \frac{2HU^i - 2/3WU^{i+3} + BU^{i+2}}{\sqrt{G_H}}dU$$

$$S_i = 2HT_i - \frac{2}{3}WT_{i+3} + BT_{i+2} \tag{4.12}$$

The integral $S_i$ is around a closed curve, and the differentiation of it will vanish:

$$\oint \frac{d}{dU}(U^{j-1}\sqrt{G_H})dU = \oint (j-1)U^{j-2}\sqrt{G_H} + \frac{BU^j}{\sqrt{G_H}} - \frac{WU^{j+1}}{\sqrt{G_H}}dU = 0$$

$$(j-1)S_{j-2} - WT_{j+1} + BT_j = 0 \quad (j \geq 1) \tag{4.13}$$

Combining the expressions (4.12) and (4.13) and let $i = j - 2$:

$$S_{j-2} = 2HT_{j-2} - \tfrac{2}{3}WT_{j+1} + BT_j$$

$$2HT_{j-2} - \tfrac{2}{3}WT_{j+1} + BT_j = \tfrac{WT_{j+1} - BT_j}{(j-1)}$$

$$T_{j+1} = \frac{6H(j-1)T_{j-2}}{W(2j+1)} + \frac{3Bj}{W(2j+1)}T_j \tag{4.14}$$

Now by using the expression (4.12) for i=0 and the expression (4.14) for j=1 and for j=2 we get:

$$S_0 = \frac{1}{5}(6HT_0 + \frac{B^2}{W}T_1) \tag{4.15}$$

Using expression (4.14) and taking values of j=1,2,3 and 4 we find $T_2, T_3, T_5$ in terms of $T_0$ and $T_1$:

$$T_2 = \frac{BT_1}{W}$$

$$T_3 = \frac{6HT_0}{5W} + \frac{6B^2T_1}{5W^2} \tag{4.16}$$

$$T_5 = \frac{60HBT_1}{7} + \frac{144B^2HT_0}{35W^2} + \frac{144B^4T_1}{35W^4}$$

By setting $\Delta H = 0$ we can find the plane where the periodic solutions can exist:

$$W(AT_3 + T_5) = 3c\tilde{s}S_0 + AT_3$$

$$W = \frac{3c\tilde{s}S_0 + AT_3}{(AT_3 + T_5)}$$

So the periodic solutions can exist at $O(\delta)$ close to the $\{W = \frac{3c\tilde{s}S_0 + AT_3}{(AT_3 + T_5)}\}$ plane. Now by setting $\Delta W = 0$ in the plane $\{W = \frac{3c\tilde{s}S_0 + AT_3}{(AT_3 + T_5)}\}$ we get

$$:\frac{T_1}{T_0} = \frac{A(1-W)}{B}, \text{ let } T(H) = \frac{T_1}{T_0} \text{ so :}$$

$$T(H, \frac{3c\tilde{s}S_0 + AT_3}{(AT_3 + T_5)}) = \frac{A}{B}(1 - \tfrac{3c\tilde{s}S_0 + AT_3}{AT_3 + T_5}) \tag{4.17}$$

As $H \uparrow H_s(= 0)$ the period of the unperturbed solution $(T_0)$ goes to infinity so $T \downarrow 0$ so (4.17) becomes:

$$\frac{A}{B}(1 - \frac{3c\tilde{s}S_0 + AT_3}{AT_3 + T_5}) = 0$$

Thus

$$AT_3 + T_5 - 3c\tilde{s}S_0 - AT_3 = 0$$

$$T_5 = 3c\tilde{s}S_0$$

By substituting (4.16) into $T_5$ and (4.15) into $S_0$:

$$\frac{60HBT_1}{7} + \frac{144B^2HT_0}{35W^2} + \frac{144B^4T_1}{35W^4} = 3c\tilde{s}\frac{1}{5}(6HT_0 + \frac{B^2}{W}T_1)$$

When the expression above is divided by $T_0$ we use again the limit of $H \uparrow H_s$, $T \downarrow 0$:

$$\frac{60HBT}{7} + \frac{144B^2H}{35W^2} + \frac{144B^4T}{35W^4} = 3c\tilde{s}\frac{1}{5}(6H + \frac{B^2}{W}T)$$

$$\frac{144B^2H}{35W^2} = \frac{18Hc\tilde{s}}{5}$$

$$W^2 = \frac{24B^2}{7c\tilde{s}}$$

and since we are looking for a homoclinic bifurcation, we focus on a unique pair $(H_0, W_0)$; the desert state we are interested in is the saddle point $\tilde{S}$ where at $W_0 = 1$. The bounded part of the stable manifold is contained in the bounded part of the unstable manifold of $\mathcal{M}_0$ when the free parameter of speed is $\tilde{s} = \frac{24B^2}{7c}$, which means that for $\tilde{s}^* = \frac{24B^2}{7c}$, there exists a homoclinic orbit to the saddle point $\tilde{S}$ for the system (1.6). This is the same outcome as the one in Chapter 3 when we used the Geometric Singlular Perturbation approach. This part of the thesis is very important since we proved with two different mathematical approaches that a homoclinic orbit exists when the speed parameter $\tilde{s}^* = \frac{24B^2}{7c}$.

## 4.3 Periodic orbits

In this section we want to find the range where the periodic orbits occur. Thus, we will go back to Chapter 1 and look at the eigenvalues, correspond the the spiral nodes, of the point $(U_+^*, P_+^*, W_+^*)$ are: $\lambda_{2,3} = \pm i\sqrt{B} + \delta(\frac{U_+^{*2}}{c} - \frac{\tilde{s}}{2})$.
When $\tilde{s} = \frac{2U_+^{*\,2}}{c}$ the real part of the eigenvalues is zero and a Hopf Bifurcation can be determined. A Hopf bifurcation occurs when a pair of complex-conjugate eigenvalues of some equilibrium point pass through the imaginary axis as the bifurcation parameter is varied, in this case parameter $\tilde{s}$ , the stability of the system changes and a periodic solution arises. After simplifying $U_+^{*2}$ using the Taylor expansion $(1+x)^{\frac{1}{2}} = 1 + \frac{x}{2} - \frac{x^2}{8}$ as $A \to \infty$, $U_+^{*2} \sim \frac{A^2}{4B^2}$ (this is the same for $U_-^{*2}$), then $\tilde{s} = \frac{2U_+^{*2}}{c}$ becomes $\tilde{s} \approx \frac{A^2}{2B^2c}$.

However the eigenvalue equation (1.9) is very similar to the eigenvalue equation of the article [13]. Sherratt uses the method of comparing the eigenvalue equation with We will use the generic form of cubic eigenvalue equation at Hopf Bifurcation to compare it with the eigenvalue equation (1.9) in order to find the Hopf bifurcation curve in the A-$\tilde{s}$ parameter plane (rainfall-speed). In our case we have the following conditions coming from the generic form, $0 = (\lambda^2 + C_1^2)(C_2\lambda + C_3) = C_2\lambda^3 + C_3\lambda^2 + C_1^2C_2\lambda + C_1^2C_3$:

$$(-A\delta + \delta\tilde{s}c - \delta U^{*2})(-A\delta^2\tilde{s} + Bc - \delta^2\tilde{s}U^{*2}) - B\delta c(U^{*2} - A) = 0 \qquad (4.18)$$

$$B(U^{*2} - A)(-A\delta + \delta\tilde{s}c - \delta U^{*2}) > 0 \qquad (4.19)$$

By using the conditions (4.18) and (4.19) and taking into account the order of $\delta$: $Bc^2\tilde{s} - BcU_+^{*2} - BcU_+^{*2} = 0$. We conclude the same result as above, $\tilde{s} = \frac{A^2}{2B^2c}$. Therefore, we conclude that there are periodic solutions if $\tilde{s}$ lies between $\frac{24B^2}{7c}$ and $\frac{A^2}{2B^2c}$.

### 4.3.1 Illustration of periodic orbits

In this section there are three figures, which sum up what happens before, at and after the homoclinic bifurcation. The phase portraits normally are in 3D as shown in figures (3.1) and (3.2). Even though, here they are exhibited in two dimensions, and only one equilibrium point from the non-hyperbolic

manifold is shown, the reason is to make the illustration and the explanation easier. We take the case of $\tilde{s} < \frac{2U_+^{*\,2}}{c}$ so the point of the non-hyperbolic manifold is an unstable spiral.

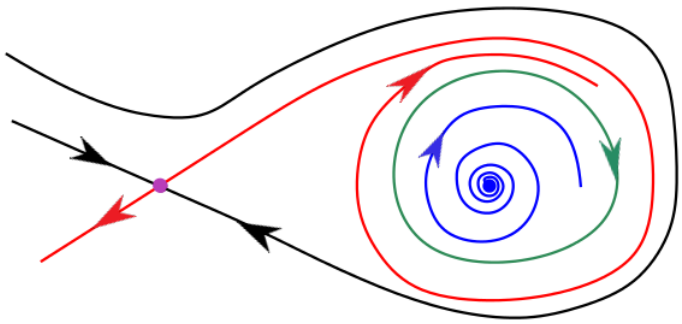

Figure 4.4: This phase portrait(of the perturbed system) is before a homoclinic bifurcation. The unstable manifold(red) of the saddle point is trapped between the stable limit cycle(green) and the stable manifold(black) of the saddle point. As the parameters values change the limit cycle is expanding and pushing outwards the two manifolds.

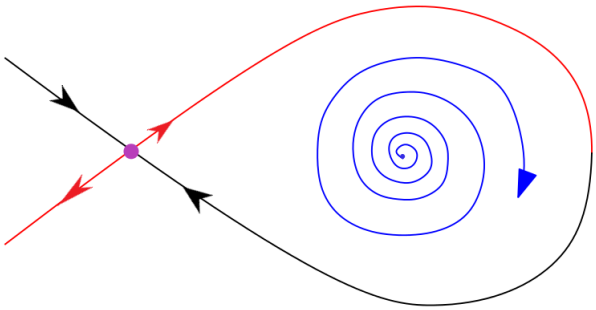

Figure 4.5: The limit cycle had a finite period but it was slowing down as it was approaching the saddle point. It coincided with the stable and unstable manifold and collided with the saddle point. Now the limit cycle has an infinite period and it's forming a homoclinic orbit.

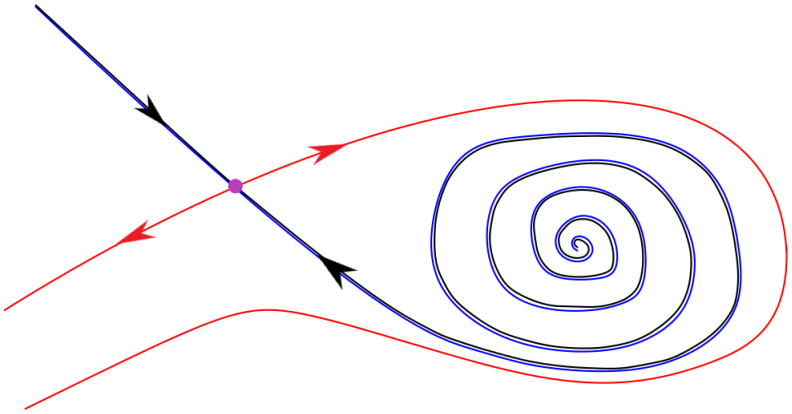

Figure 4.6: This is the phase portrait after the homoclinic bifurcation where the stable manifold is coincide with the spiral and the limit cycle degenerated.

The issue here is that in these figures, we assumed without proving that the limit cycle, trapped between the stable and the unstable manifold of the saddle point, is stable. Apart from this issue all the Figures above are represented in a 2D- plane for simplified explanation. Thus, the next chapter of the thesis is dedicated on the mathematical procedure which must followed to determine the stability of periodic orbits.

# Chapter 5

# Stability of periodic solutions

In Chapters 3 and 4 we showed that for a unique value of the speed parameter $\tilde{s} = \tilde{s}^*$ there exists a homoclinic orbit emerging from the intersection of the stable and unstable manifold of the saddle point. We also showed that for a unique value of $\tilde{s}$ the system changes stability and a Hopf bifurcation occurs. That means near $\tilde{s} = \frac{A^2}{2B^2c}$ the system has periodic solutions. In this section, we aim to determine the stability characteristics of the periodic orbits near the Hopf bifurcation. Floquet theory and specifically the Floquet multipliers is the mathematical "tool" we will use in order to find the stability of these periodic solutions. However, (1.6) is a three-dimensional ODE system, which is quite complicated to apply directly the Floquet theory. This part of the thesis includes an intermezzo section where it explains how can we find the Floquet multipliers near a Hopf bifurcation in a two dimensional system. This procedure will help us understand how the stability analysis can be applied in a three-dimensional system.
Below is the definition of Floquet multipliers and the Floquet theorem [10], which will be needed later on.

## 5.1 Floquet theory

Consider the n-dimensional system of ODEs,

$$\dot{\boldsymbol{x}} = A(t)\boldsymbol{x} \tag{5.1}$$

where A is a periodic matrix, $A(t) = A(t+T)$. The equations of this form (5.1) occur as the linearization of the dynamics about a periodic orbit of period T.

According to Floquet [10], in order to solve (5.1), we consider a matrix differential equation $\frac{d}{dt}\Phi = A(t)\Phi$, $\Phi(t_0, t_0) = I$.
The general solution is represented in terms of the fundamental matrix $\Phi(t, t_0)$. When A is constant we can use the method of "exponential matrices" to find the solution; $\Phi(t, t_0) = e^{(t-t_0)A}$. However this method doesn't work for time depended cases because when $\Phi(t, t_0) = e^{\int_{t_0}^{t} A(s)ds}$, $A(s_1)$ doesn't commute with $A(s_2)$ when $s_1 \neq s_2$.
An important quantity of the fundamental matrix $\Phi$ at one period T, is the *Monodromy matrix*: $M = \Phi(T, 0)$.
Given now that the initial conditions are $x(0) = x_0$, then $x(T) = Mx_0$. The eigenvalues of $M$ are called the **Floquet multipliers** or characteristic multipliers, and suppose $x_0$ is an eigenvector of $M$ with eigenvalue $\mu$, then

$$x(nT) = \mu^n x_0 = e^{n \ln \mu} x_0$$

The exponent $ln\mu$ is called a *Floquet exponent* or characteristic exponent.

**Theorem 5.1** [10]: Suppose $\dot{\boldsymbol{x}} = A(t)\boldsymbol{x}$ has characteristic multipliers $\mu_i$ and exponents $\lambda_i$, $(\mu_i = e^{\lambda_i T})$. Then

$$\begin{aligned} \mu_1\mu_2...\mu_n &= e^{\int_0^T Trace(A(t))dt} \\ \lambda_1 + \lambda_2 + ... + \lambda_n &= \tfrac{1}{T}\int_0^T Tr(A(t))dt \end{aligned} \tag{5.2}$$

**Floquet Theorem 1883** [10]: Let $M$ be the monodromy matrix for a T-periodic linear system (5.1) and $TB = lnM$ its logarithm. Then there exists a T-periodic matrix $P$ such that the fundamental matrix solution is $\phi(t, 0) = Pe^{tB}$.
*Note: By using the information above we can deduce that the eigenvalues of $e^{TB}$ are the Floquet multipliers.*

There are some important conditions regarding the stability of the periodic orbits:

1. The monodromy matrix $M$ of a linearised system (5.1) about a periodic orbit always has at least one unit eigenvalue.

2. If the real part of all characteristic exponents of (5.1) is negative or if all of its multipliers apart from the trivial unit multiplier have magnitude strictly less than one, $|\mu_i| < 1$, then the periodic solution is asymptotically stable.(Theorem of asymptotic linear stability)

3. If the real part of at least one of the the characteristic exponents of (5.1) is positive then there is instability.

# Intermezzo

We introduce this new model problem:

$$\ddot{x} + \alpha\mu\dot{x} + x = \beta_{30}x^3 + \beta_{21}\dot{x}x^2 + \beta_{12}\dot{x}^2x + \beta_{03}\dot{x}^3 \tag{5.3}$$

where $\dot{} = \frac{d}{dt}$, $\alpha < 0$ and $\beta_{30}, \beta_{31}\, \beta_{12}, \beta_{03}$ are arbitrary constants.
*Note: At this point the interpretation of $\alpha$ is not clear, however it will play an important role in the upcoming analysis.*
Let $\dot{x} = y$ then the system (5.3) becomes:

$$\begin{aligned} \dot{x} &= y \\ \dot{y} &= \beta_{30}x^3 + \beta_{31}\dot{x}x^2 + \beta_{12}\dot{x}^2x + \beta_{03}\dot{x}^3 - x - \alpha\mu y \end{aligned} \tag{5.4}$$

When $\dot{x} = \dot{y} = 0$, the origin is an equilibrium point. The Jacobian matrix at the origin is:

$$J = \begin{pmatrix} 0 & 1 \\ -1 & -\alpha\mu \end{pmatrix}$$

so the eigenvalues are $\lambda_{1,2} = \frac{1}{2}(-\alpha\mu \pm \sqrt{\alpha^2\mu^2 - 4})$.

- For $\mu > 0$, $\mathrm{Re}(\lambda) > 0$ and when $\sqrt{\alpha^2\mu^2 - 4} < |\alpha\mu| \Rightarrow$ unstable
- For $\mu < 0$, $\mathrm{Re}(\lambda) < 0$ and when $\sqrt{\alpha^2\mu^2 - 4} < |\alpha\mu| \Rightarrow$ stable
- The spirals occur when $\alpha^2\mu^2 - 4 < 0$, otherwise the equilibrium point is a node

- For $\mu = 0$, $\mathrm{Re}(\lambda) = 0$ so the eigenvalues are $\lambda_{1,2} = \pm i$, therefore $\mu = 0$ is a Hopf bifurcation point.

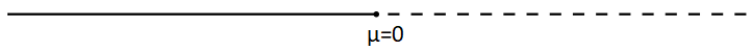


Figure 5.1: 1D-Parameter plane for $\mu$, where —is stable, - - - is unstable

To find the solutions of (5.3) we will use a method which constructs the solutions near a bifurcation value $\mu = \mu_b = 0$. This means that we are going to study what happens to the solution when $\epsilon = \mu - \mu_b$, in this case $\epsilon = \mu$ [6]. Assuming that $y = y_s = 0$ is the steady state found above, then $x$ can be expanded as $x \sim y_s + e^{\gamma} y$. By substituting $\mu = \epsilon$ and $x = \epsilon^{\gamma} y$ into (5.3) and by balancing the terms $O(\epsilon)$ with $O(\epsilon^{2\alpha})$, we find that $\gamma = \frac{1}{2}$, so the equation (5.3) becomes:

$$\begin{aligned} \sqrt{\epsilon}(\ddot{y} + \epsilon\alpha\dot{y} + y) &= \epsilon\sqrt{\epsilon}(\beta_{30}y^3 + \beta_{21}\dot{y}y^2 + \beta_{12}\dot{y}^2 y + \beta_{03}\dot{y}^3) \\ \ddot{y} + y &= \epsilon(\beta_{30}y^3 + \beta_{21}\dot{y}y^2 + \beta_{12}\dot{y}^2 y + \beta_{03}\dot{y}^3 - \alpha\dot{y}) \end{aligned} \tag{5.5}$$

Applying the method of averaging will help us find a more accurate approximation of a solution of a system when there is a perturbation parameter $\epsilon$, the standard perturbation expansion is not suitable because it gives secular terms and as t$\to \infty$ the system will diverge. According to F.Verhulst [15], two theorems should be satisfied in order to apply the method of averaging.
Consider the equation:

$$\dot{x} = \epsilon f(t, x) + \epsilon^2 g(t, x, \epsilon) \tag{5.6}$$

with $x \in D \subset \mathbf{R}^n, t \geq 0$. Moreover we assume that both $f(t, x)$ and $g(t, x, \epsilon)$ are T-periodic in t. Separately we consider in $D$ the averaged equation

$$\dot{y} = \epsilon f^0(y) \tag{5.7}$$

Under certain conditions, equilibrium solutions of the averaged equation turn out to correspond with T-periodic solutions of equation (5.6).

**Theorem 5.2:**
Consider the equation (5.6) and suppose that:

a. the vector functions $f, g, \partial f/dx, \partial^2 f/\partial x^2$ are defined, continuous and bounded by a constant $M$ (independent of $\epsilon$) in $[0, \infty) \times D, 0 \leq \epsilon \leq \epsilon_0$;

b. $f$ and $g$ are T-periodic in t (T independent of $\epsilon$)

If $p$ is a critical point of the averaged equation (5.7) whereas

$$|\partial f^0(y)/\partial y|_{y=p} \neq 0 \tag{5.8}$$

$\partial f^0(y)/\partial y$ is a matrix, then there exists a T-periodic solution $\phi(t, \epsilon)$ of equation (5.6) which is close to p such that

$$\lim_{\epsilon \to 0} \phi(t, \epsilon) = p.$$

**Theorem 5.3**:
Consider the equation (5.6) and suppose that the conditions of Theorem 5.2 have been satisfied. If the eigenvalues of the critical point $y = p$ of the averaged equation (5.7) all have negative real parts, the corresponding periodic solution $\phi(t, \epsilon)$ of equation (5.6) is asymptotically stable for sufficiently small $\epsilon$ . If one of the eigenvalues has positive real part, $\phi(t, \epsilon)$ is unstable.

The Theorem 5.3 and by following the Floquet theory above, will help us understand how the Floquet multipliers can be found.
From the Theorem 5.3 [15], the trace of the matrix B is the sum of the characteristic exponents, trB= $\lambda_1 + \lambda_2 = \Lambda_1 + \Lambda_2$. And from the Floquet theorem we know that there is at least one characteristic exponent equal to 0 about a periodic orbit of a linearized system.
Now going back to the model problem and the equation (5.5). Combining the method of multiple scales and the method of averaging ([6],[7]), we introduce a new time variable $\tilde{t} = (1 + \epsilon\nu)t$. By introducing this new time scale the slow time scale will minimize the error in the approximation. We are looking for solutions which are periodic with period $T = \frac{2\pi}{\tilde{t}}$, therefore equation (5.5)

needs to be transformed into a system with respect to $\tilde{t}$. The chain rule gives the first and second derivative:

$$\begin{aligned}\frac{d}{dt} &= \frac{d}{d\tilde{t}}\frac{d\tilde{t}}{dt} = (1+\epsilon\nu)\frac{d}{d\tilde{t}} \\ \frac{d^2}{dt^2} &= \frac{d}{dt}(\frac{d}{d\tilde{t}}\frac{d\tilde{t}}{dt}) = (1+\epsilon\nu)^2\frac{d^2}{d\tilde{t}^2}\end{aligned} \tag{5.9}$$

Substitute the derivatives (5.9) into (5.5):

$$\begin{aligned}&(1+\epsilon\nu)^2\frac{d^2y}{d\tilde{t}^2} + y = \epsilon[\beta_{30}y^3 + \beta_{21}(1+\epsilon\nu)\frac{dy}{d\tilde{t}}y^2 + \beta_{12}(1+2\epsilon\nu+\epsilon^2\nu^2)(\frac{dy}{d\tilde{t}})^2y + \\ &\beta_{03}(1+\epsilon\nu)^3(\frac{dy}{d\tilde{t}})^3 - \alpha(1+\epsilon\nu)\frac{dy}{d\tilde{t}}]\end{aligned} \tag{5.10}$$

After dividing the equation (5.10) with $(1+\epsilon\nu)$ and using the Taylor expansion of $(1-x)^{-2} = 1+2x+3x^2$ we get:

$$\begin{aligned}&\ddot{y} + (1+\epsilon\nu)^{-2}y = \epsilon(1+\epsilon\nu)^{-2}[\beta_{30}y^3 + \beta_{21}(1+\epsilon\nu)\dot{y}y^2 + \\ &\beta_{12}(1+2\epsilon\nu+\epsilon^2\nu^2)(\dot{y})^2y + \beta_{03}(1+\epsilon\nu)^3(\dot{y})^3 - \alpha(1+\epsilon\nu)\dot{y}] \\ &\ddot{y} + y - 2\epsilon\nu y = \epsilon[\beta_{30}y^3 + \beta_{21}\dot{y}y^2 + \beta_{12}(\dot{y})^2y + \beta_{03}(\dot{y})^3 - \alpha\dot{y}] + O(\epsilon^2) \\ &\ddot{y} + y = \epsilon[\beta_{30}y^3 + \beta_{21}\dot{y}y^2 + \beta_{12}(\dot{y})^2y + \beta_{03}(\dot{y})^3 - \alpha\dot{y} + 2\nu y]\end{aligned} \tag{5.11}$$

When $\epsilon = 0$, $\ddot{y} + y = 0$ the general solution is :

$$y(\tilde{t}) = r(\tilde{t})\cos(\tilde{t} + \psi(\tilde{t})) \tag{5.12}$$

where the amplitude $r$ and the phase $\psi$ are functions of time. Differentiate the solution (5.12):

$$\begin{aligned}\dot{y} &= -r(\tilde{t})\sin(\tilde{t}+\psi(\tilde{t})) \\ \ddot{y} &= -\dot{r}\sin(\tilde{t}+\psi(\tilde{t})) - r(1+\dot{\psi})\cos(\tilde{t}+\psi(\tilde{t}))\end{aligned} \tag{5.13}$$

and the substitution of these expressions (5.13) into (5.11) produces an equation of r and $\psi$:

$$\begin{aligned}&-\dot{r}\sin(\tilde{t}+\psi(\tilde{t})) - \dot{\psi}r\cos(\tilde{t}+\psi(\tilde{t})) = \epsilon[\beta_{30}r^3\cos^3(\tilde{t}+\psi(\tilde{t})) - \\ &\beta_{21}r^3\cos^2(\tilde{t}+\psi(\tilde{t}))\sin(\tilde{t}+\psi(\tilde{t})) + \beta_{12}r^3\sin^2(\tilde{t}+\psi(\tilde{t}))\cos(\tilde{t}+\psi(\tilde{t})) - \\ &\beta_{03}r^3\sin^3(\tilde{t}+\psi(\tilde{t})) + \alpha r\sin(\tilde{t}+\psi(\tilde{t})) + 2r\nu\cos(\tilde{t}+\psi(\tilde{t}))]\end{aligned} \tag{5.14}$$

and the phase-amplitute coordinates are:

$$\begin{aligned}
&\dot{r} = -\epsilon \sin(\tilde{t}+\psi(\tilde{t}))[\beta_{30} r^3 \cos^3(\tilde{t}+\psi(\tilde{t})) - \beta_{21} r^3 \cos^2(\tilde{t}+\psi(\tilde{t})) \sin(\tilde{t}+\psi(\tilde{t}))+ \\
&\beta_{12} r^3 \sin^2(\tilde{t}+\psi(\tilde{t})) \cos(\tilde{t}+\psi(\tilde{t})) - \beta_{03} r^3 \sin^3(\tilde{t}+\psi(\tilde{t}))+ \\
&\alpha r \sin(\tilde{t}+\psi(\tilde{t})) + 2r\nu \cos(\tilde{t}+\psi(\tilde{t}))] \\
&\\
&\dot{\psi} = -\epsilon \cos(\tilde{t}+\psi(\tilde{t}))[\beta_{30} r^2 \cos^3(\tilde{t}+\psi(\tilde{t})) - \beta_{21} r^2 \cos^2(\tilde{t}+\psi(\tilde{t})) \sin(\tilde{t}+\psi(\tilde{t}))+ \\
&\beta_{12} r^2 \sin^2(\tilde{t}+\psi(\tilde{t})) \cos(\tilde{t}+\psi(\tilde{t})) - \beta_{03} r^2 \sin^3(\tilde{t}+\psi(\tilde{t}))+ \\
&\alpha \sin(\tilde{t}+\psi(\tilde{t})) + 2\nu \cos(\tilde{t}+\psi(\tilde{t}))]
\end{aligned} \tag{5.15}$$

Using the trigonometric identities of $\cos^2\theta = \frac{1}{2}(1+\cos 2\theta)$ and $\sin^2\theta = \frac{1}{2}(1-\cos 2\theta)$ the phase - amplitude coordinates now are:

$$\begin{aligned}
&\dot{r} = -\epsilon[\beta_{30} r^3 \cos^3(\tilde{t}+\psi(\tilde{t})) \sin(\tilde{t}+\psi(\tilde{t})) - \tfrac{\beta_{21}}{8} r^3 (1-\cos 4(\tilde{t}+\psi(\tilde{t})))+ \\
&\beta_{12} r^3 \sin^3(\tilde{t}+\psi(\tilde{t})) \cos(\tilde{t}+\psi(\tilde{t})) - \tfrac{\beta_{03}}{8} r^3 (3+\cos 4(\tilde{t}+\psi(\tilde{t})) - 4\cos 2(\tilde{t}+\psi(\tilde{t})))+ \\
&\tfrac{\alpha r}{2}(1-\cos 2(\tilde{t}+\psi(\tilde{t}))) + 2\nu r \cos(\tilde{t}+\psi(\tilde{t})) \sin(\tilde{t}+\psi(\tilde{t}))] \\
&\\
&\dot{\psi} = -\epsilon[\tfrac{\beta_{30}}{8} r^2 (3+\cos 4(\tilde{t}+\psi(\tilde{t})) + 4\cos 2(\tilde{t}+\psi(\tilde{t})))- \\
&\beta_{21} r^2 \cos^3(\tilde{t}+\psi(\tilde{t})) \sin(\tilde{t}+\psi(\tilde{t})) + \tfrac{\beta_{12}}{8} r^2 (1-\cos 4(\tilde{t}+\psi(\tilde{t})))- \\
&\beta_{03} r^2 \sin^3(\tilde{t}+\psi(\tilde{t})) \cos(\tilde{t}+\psi(\tilde{t})) + \alpha \sin(\tilde{t}+\psi(\tilde{t})) \cos(\tilde{t}+\psi(\tilde{t}))+ \\
&\nu(1+\cos 2(\tilde{t}+\psi(\tilde{t})))]
\end{aligned} \tag{5.16}$$

and after averaging over $\tilde{t}$

$$\begin{aligned}
\frac{dr_a}{d\tilde{t}} &= \epsilon\left(\frac{\beta_{21} r_a^3}{8} + \frac{3\beta_{03} r_a^3}{8} - \frac{\alpha r_a}{2}\right) \\
\frac{d\psi_a}{d\tilde{t}} &= \epsilon\left(-\frac{3\beta_{30} r_a^2}{8} - \frac{\beta_{12} r_a^2}{8} - \nu\right).
\end{aligned} \tag{5.17}$$

The critical points of the equations (5.17) can be found when $\frac{dr_a}{d\tilde{t}} = \frac{d\psi_a}{d\tilde{t}} = 0$:

$$\begin{aligned}
&\tfrac{\epsilon}{2} r_a^*\left(\frac{\beta_{21} r_a^{2*}}{4} + \frac{3\beta_{03} r_a^{2*}}{4} - \alpha\right) = 0 \\
&r_a^* = \sqrt{\frac{4\alpha}{\beta_{21}+3\beta_{03}}}, 0
\end{aligned} \tag{5.18}$$

That means, if the initial value of the amplitude $r_0$ is $\sqrt{\frac{4\alpha}{\beta_{21}+3\beta_{03}}}$ or 0, then the amplitude $r_a$ is constant for all time. Although, at this point we take

$r_a^* = \sqrt{\dfrac{4\alpha}{\beta_{21}+3\beta_{03}}} = p$, since $r_a^* = 0$ gives $y = 0$ which is not a periodic solution. However, for $r_a^* = \sqrt{\dfrac{4\alpha}{\beta_{21}+3\beta_{03}}}$ to be a real number we assume that $\beta_{21} + 3\beta_{03} < 0$, since $\alpha < 0$.
Now letting $\dfrac{d\psi_a}{d\tilde{t}} = 0$:

$$-\epsilon(\frac{r_a^{2*}}{8}(3\beta_{30}+\beta_{12})+\nu) = 0 \tag{5.19}$$

Thus, we indeed have a critical point of the averaged equations if we set:

$$\nu = -\frac{\alpha(3\beta_{30}+\beta_{12})}{2(\beta_{21}+3\beta_{03}}) \tag{5.20}$$

But $\psi_a^*$ is not determined uniquely under these conditions, so we let $\psi_a^* = \psi_0$. And the Jacobian matrix of the system (5.17) around the amplitude $r_a^* = \sqrt{\dfrac{4\alpha}{\beta_{21}+3\beta_{03}}}$ which corresponds to the periodic solution, is:

$$\begin{pmatrix} \epsilon(\frac{3}{8}(\beta_{21}+3\beta_{03})r_a^{2*} - \frac{\alpha}{2}) & 0 \\ 0 & 0 \end{pmatrix} = \begin{pmatrix} \epsilon\alpha & 0 \\ 0 & 0 \end{pmatrix} \tag{5.21}$$

The eigenvalues of the matrix (5.21) are $\Lambda_1 = 0$ and $\Lambda_2 = \epsilon\alpha$. According to the Floquet theory and Theorem 5.3, these eigenvalues are the characteristic exponents, therefore the characteristic multipliers will be : $\mu_1 = e^0 = 1$ and $\mu_2 = e^{\epsilon\alpha}$. The Floquet multiplier $\mu_1$ satisfies the first condition, a linearised system around a periodic orbit has at least one unit eigenvalue and the other multiplier $|\mu_2| < 1$, since $\alpha < 0$, leads to condition 2, where the periodic solution is asymptotically stable, which yields the existence of a $2\pi$ periodic solution in $\tilde{t}$.
When $r_a^* = \sqrt{\frac{4\alpha}{\beta_{21}+3\beta_{03}}}$ the periodic solution is:

$$y(\tilde{t}) = \sqrt{\frac{4\alpha}{\beta_{21}+3\beta_{03}}}\cos(\tilde{t}+\psi_0) + O(\epsilon) \tag{5.22}$$

We can also obtain general solution for the periodic orbits by solving the first equation of (5.17) by separation of variables. Using the method of partial

fractions (5.17) yields:

$$\int -\frac{2}{\epsilon\alpha r_a} + \frac{\sqrt{(\beta_{21}+3\beta_{03})}}{\epsilon\alpha}\left(\frac{1}{\sqrt{(\beta_{21}+3\beta_{03})}r_a - 2\sqrt{\alpha}} + \frac{1}{\sqrt{(\beta_{21}+3\beta_{03})}r_a + 2\sqrt{\alpha}}\right)dr_a = \int d\tilde{t} \tag{5.23}$$

Solving the integral gives:

$$\frac{1}{\epsilon\alpha}\left(-2log(r_a) + log(\sqrt{(\beta_{21}+3\beta_{03})}r_a - 2\sqrt{\alpha}) + log(\sqrt{(\beta_{21}+3\beta_{03})}r_a + 2\sqrt{\alpha})\right. = \tilde{t} + c \tag{5.24}$$

So that

$$log(\frac{1}{r_a^2}) + log((\beta_{21}+3\beta_{03})r_a^2 - 4\alpha) = \epsilon\alpha(\tilde{t}+c) \tag{5.25}$$

When $\tilde{t} = 0$, the initial value of the amplitude is $r_0$, substitute $r(0) = r_0$ into (5.25) we can find the arbitrary constant c:

$$\epsilon\alpha c = log(\frac{(\beta_{21}+3\beta_{03})r_0^2 - 4\alpha}{r_0^2}) \tag{5.26}$$

Then equation (5.25) becomes:

$$log[(\frac{(\beta_{21}+3\beta_{03})r_a^2 - 4\alpha}{r_a^2})(\frac{r_0^2}{(\beta_{21}+3\beta_{03})r_0^2 - 4\alpha})] = \epsilon\alpha\tilde{t}$$

$$r_a^2 = \frac{4\alpha r_0^2}{(\beta_{21}+3\beta_{03})r_0^2(1-e^{\epsilon\alpha\tilde{t}}) + 4\alpha e^{\epsilon\alpha\tilde{t}}} \tag{5.27}$$

$$r_a = \pm\frac{2r_0\sqrt{\alpha}e^{\frac{-\epsilon\alpha\tilde{t}}{2}}}{\sqrt{(\beta_{21}+3\beta_{03})r_0^2(e^{-\epsilon\alpha\tilde{t}}-1)+4\alpha}}$$

The general solution of the original system can thus be approximated by:

$$y(\tilde{t}) = \pm\frac{2r_0\sqrt{\alpha}e^{\frac{-\epsilon\alpha\tilde{t}}{2}}}{\sqrt{(\beta_{21}+3\beta_{03})r_0^2(e^{-\epsilon\alpha\tilde{t}}-1)+4\alpha}}\cos(\tilde{t}+\psi_0) + O(\epsilon). \tag{5.28}$$

There is another method which can define the stability of a unique limit cycle

near the Hopf bifurcation point but it's not possible to find an approximate expression of the periodic solution like above [7]. This method is by applying the Hopf Bifurcation Theorem [9] which is stated below.

**Hopf Bifurcation Theorem**
Let $\dot{x} = f(x, y; \mu)$ and $\dot{y} = g(x, y; \mu)$ in $\mathbf{R}^2$.
Suppose that the following hold:

1. $f(0, 0, \mu) = g(0, 0, \mu) = 0$ for all $\mu \in [-\mu_0, \mu_0]$, for some $\mu_0 > 0$
   (*Note: the origin is an equilibrium point provided the parameter $\mu$ lies in some interval that includes $\mu = 0$*)

2. the Jacobian matrix, evaluated at the origin, with $\mu = 0$, is

   $$\begin{pmatrix} 0 & -\omega \\ \omega & 0 \end{pmatrix}$$

   for some real constant $\omega \neq 0$
   (*When $\mu = 0$, the Jacobian matrix of the linearisation about the origin has eigenvalues $\lambda_{1,2} = \pm i\omega$, so at $\mu = 0$ the origin is a center*)

3. the eigenvalues of the equilibrium point at the origin are a complex-conjugate pair for $\mu \in [-\mu_0, \mu_0]$ given by $\alpha(\mu) \pm i\beta(\mu)$, with $\alpha(\mu)$ and $\beta(\mu)$ real value functions of the parameter $\mu$.

4. $a \neq 0$ where

   $a = \frac{1}{16}(f_{xxx} + g_{xxy} + f_{xyy} + g_{yyy}) + \frac{1}{16\omega}[f_{xy}(f_{xx} + f_{yy}) - g_{xy}(g_{xx} - g_{yy}) - f_{xx}g_{xx} + f_{yy}g_{yy}]$

   with all these partial derivatives evaluated at $\mu = 0$.

Then:

A) If $a\alpha'(0) < 0$, a unique limit cycle bifurcates from the origin in $\mu > 0$ as $\mu$ passes through 0.
   The stability of the limit cycle [in $\mu > 0$] is the same as the stability of the origin in $\mu < 0$.

B) If $a\alpha'(0) > 0$, a unique limit cycle bifurcates from the origin in $\mu < 0$ as $\mu$ passes through 0.
The stability of the limit cycle [in $\mu < 0$] is the same as the stability of the origin in $\mu > 0$.

In the case of the model problem (5.3), $f(x, y, \mu) = y$ and $g(x, y, \mu) = \beta_{30}x^3 + \beta_{31}\dot{x}x^2 + \beta_{12}\dot{x}^2x + \beta_{03}\dot{x}^3 - x - \alpha\mu y$, therefore the steps 1 and 2 of the Hopf Bifurcation Theorem hold, with $\omega = -1$.
Step 3: The eigenvalues can be expressed as $\alpha(\mu) \pm i\beta(\mu) = -\frac{1}{2}\alpha\mu \pm \frac{i}{2}\sqrt{4 - \alpha^2\mu^2}$

Step 4: The partial derivatives are calculated when $x = y = \mu = 0$

$$f_x = 0, \quad f_{xx} = 0, \quad f_{xxx} = 0, \quad f_{xy} = 0, \quad f_{xyy} = 0, \quad f_y = 1, \, f_{yy} = 0$$

$$g_x = -1 + 3\beta_{30}x^2 + 2\beta_{21}yx + \beta_{12}y^2, \quad g_{xx} = 6\beta_{30}x + 2\beta_{21}y = 0$$

$$g_{xy} = 2\beta_{21}x + 2\beta_{12}y = 0, \quad g_{xxy} = 2\beta_{21}, \quad g_y = \beta_{21}x^2 + 2\beta_{12}yx + 3\beta_{03}y^2 - \alpha\mu$$

$$g_{yy} = 2\beta_{12}x + 6\beta_{03}y = 0 \quad g_{yyy} = 6\beta_{03}$$

Therefore, $a = \frac{1}{16}(2\beta_{21} + 6\beta_{03}) = \frac{\beta_{21}+3\beta_{03}}{8} < 0$ (as stated above $\beta_{21} + 3\beta_{03} < 0$ in order $r_a$ to be real) and $a\alpha'(0) = -\frac{\alpha}{2} \times \frac{\beta_{21}+3\beta_{03}}{8} < 0$ since $\alpha < 0$ and $\beta_{21} + 3\beta_{03} < 0$, then the condition (A) is satisfied. A unique limit cycle exists for $\mu > 0$, there is an agreement with the above procedure of method of averaging, since we chose the perturbation parameter $\epsilon$ to be positive. And the stability of the limit cycle is stable which is the same as the origin for $\mu < 0$ as shown in Figure (5.2) [11].

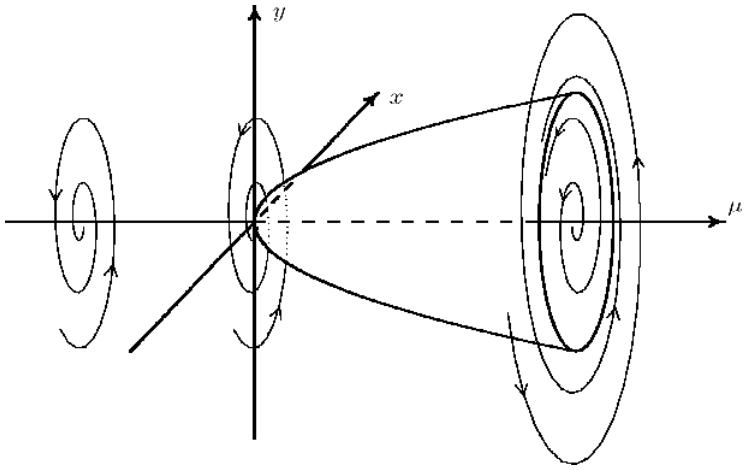


Figure 5.2: Bifurcation diagram: Supercritical Hopf Bifurcation with a stable limit cycle and unstable spiral for $\mu > 0$.

## 5.2 The Hopf and Center Manifold Theorems

In the previous section we examined the stability of periodic orbits in 2D examples, but since we study the Klausmeier model we are interested in the application of Intermezzo's techniques in 3D systems . In order to do that, we need to follow a procedure related to the Hopf Theorem in $R^n$ and the Center Manifold Theorem.

**The Hopf Theorem in $R^n$**
Let $X_\mu$ be a $C^{k+1}$, $k \geq 4$, vector field on $R^n$ such that $X_\mu(0) = 0$ for all $\mu$ and $X = (X_\mu, 0)$ is also $C^k$. Let $dX_\mu(0,0)$ have two complex conjugate eigenvalues $\lambda(\mu)$ and $\overline{\lambda(\mu)}$ such that for $\mu > 0$ $Re(\lambda) > 0$ and $\frac{d(Re(\lambda))}{d\mu}|_{\mu=0}$. We assume that the rest of the spectrum is distinct from these two eigenvalues. Then

(A) there is a $C^{k-2}$ function $\mu : (-\epsilon, \epsilon) \to R$ such that $(X_1, 0, \mu(X_1))$ is on closed orbit of period $2\pi/|\lambda(0)|$ and radius growing like $\sqrt{\mu}$ of X for $X_1 \neq 0$ and such that $\mu(0) = 0$ and this conclusion is true.

(B) There is a neighbourhood U of (0,0,0) in $R^3$ such that any closed orbit in U is one of those above. If 0 is an attractor for $X_0$, then

(C) $\mu(X_1) > 0$ for all $X_1 \neq 0$ and the orbits are attracting.

Conclusion (B) is true if the rest of the spectrum remains in the left half plane as $\mu$ crosses 0, and conclusion (C) is true if relative to $\lambda(\mu)$, $\overline{\lambda(\mu)}$,0 is an attractor and if when the coordinates are chosen so that:

$$dX_0(0) = \begin{pmatrix} 0 & |\lambda(\mu)| & d_3X^1(0) \\ -|\overline{\lambda(\mu)}| & 0 & d_3X^2(0) \\ 0 & 0 & d_3X^3(0) \end{pmatrix}, \lambda(0) \notin \sigma(d_3X^3(0)) \tag{5.29}$$

where $\lambda(0) \notin \sigma(d_3X^3(0))$ is independent of the way $R^n$ is split into a space corresponding to the $\lambda(\mu)$, $\overline{\lambda(\mu)}$ and a complementary one since choosing a different complementary subspace will only replace $d_3X^3(0)$ by a conjugate operator : $cd_3X^3(0)c^{-1}$.

**Center Manifold Theorem:** Suppose that f is a $C^k$ vector field, $k \geq 1$, with a fixed point at the origin. Let the eigenspaces of $Df(0) = A$ be written $E^u \oplus E^c \oplus E^s$. Then there is a neighborhood of the origin in which there exist $C^k$ invariant manifolds: the local stable manifold, $W_loc^s$, tangent to $E^s$, on which $|x(t)| \to 0$ as $t \to \infty$, the local unstable manifold $W_loc^u$, tangent to $E^u$, on which $|x(t)| \to 0$ as $t \to -\infty$, and a local center manifold $W^c$, tangent to $E^c$.

Therefore the next step is to transform the system (1.6) where the coordinates will be chosen to have the standard form of (5.29) and the fixed point to be the origin.

Step 1: We are interested in the stability of the periodic orbit close to where the Hopf bifurcation occurs, so we will focus on the spiral points and specifically to the steady state: $(U_+^*, P_+^*, W_+^*) = (\frac{A + \sqrt{A^2 - 4AB^2}}{2B}, 0, \frac{2B^2}{A + \sqrt{A^2 - 4AB^2}})$. According to the Center Manifold Theorem the fixed point is the origin, thus we introduce the following translation of coordinates:

$$\begin{aligned} U &= \tilde{U} + U_+^* \\ P &= \tilde{P} + P_+^* \\ W &= \tilde{W} + W_+^* \end{aligned} \tag{5.30}$$

And the system (1.6) becomes:

$$\begin{aligned}
\dot{\tilde{U}} &= \tilde{P} \\
\dot{\tilde{P}} &= B(\tilde{U}+U_+^*) - (\tilde{W}+W_+^*)(\tilde{U}+U_+^*)^2 - \delta\tilde{s}\tilde{P} \\
\dot{\tilde{W}} &= \tfrac{\delta}{c}[A(\tilde{W}+W_+^*-1) + (\tilde{W}+W_+^*)(\tilde{U}+U_+^*)^2)]
\end{aligned} \tag{5.31}$$

Step 2: In this step we will find the eigenvectors corresponding to each eigenvalue of the steady state $(U_+^*, P_+^*, W_+^*)$.
(*Note: We will focus on the non-translated coordinates for algebraic simplicity and to show the complexity even without translating the coordinates*).
Since the system has the perturbation term $\delta$ we have to split the Jacobian matrix into the leading order and O($\delta$).:

$$J = \begin{pmatrix} 0 & 1 & 0 \\ B - 2W_+^*U_+^* & 0 & -U_+^{*\,2} \\ 0 & 0 & 0 \end{pmatrix} + \delta \begin{pmatrix} 0 & 0 & 0 \\ 0 & -\tilde{s} & 0 \\ 2W_+^*U_+^*/c & 0 & (A+U_+^{*\,2})/c \end{pmatrix}$$

Consider a particular eigenvector $U_0$ of J where $\lambda_0$ is the corresponding eigenvalue. Hence, at the leading order $JU_0 = \lambda_0 U_0$ and including O($\delta$) the equation becomes $(J+\delta J)(U_0+\delta U_1) = (\lambda_0+\delta\lambda_1)(U_0+\delta U_1)$ through the standard perturbation expansion.
We chose a simple steady state (0,0,1) and its eigenvalue $\lambda = 0 + \delta\frac{A}{c}$ just to show the algebra we need to follow:

$$\begin{pmatrix} 0 & 1 & 0 \\ B & -\delta\tilde{s} & 0 \\ 0 & 0 & \delta A/c \end{pmatrix} \begin{pmatrix} U_0+\delta U_1 \\ P_0+\delta P_1 \\ W_0+\delta W_1 \end{pmatrix} = \delta\frac{A}{c} \begin{pmatrix} U_0+\delta U_1 \\ P_0+\delta P_1 \\ W_0+\delta W_1 \end{pmatrix}$$

We get the following equations:
$P_0 + \delta P_1 = \delta\frac{A}{c}(U_0+\delta U_1)$
$B(U_0+\delta U_1) - \delta\tilde{s}(P_0+\delta P_1) = \delta\frac{A}{c}(P_0+\delta P_1)$
$\delta\frac{A}{c}(W_0+\delta W_1) = \delta\frac{A}{c}(W_0+\delta W_1)$
At O(1): $P_0 = 0, BU_0 = 0$
At O($\delta$): $P_1 = \frac{A}{c}U_0$ so $P_1 = 0$
$BU_1 - \tilde{s}P_0 = \frac{A}{c}P_0$ so $U_1 = 0$
$\frac{A}{c}W_0 = \frac{A}{c}W_0$, let $W_0 = 1$
At O($\delta^2$): $\frac{A}{c}W_1 = \frac{A}{c}W_1$. so $W_1 = 1$.

By following the above calculations we can find the eigenvector matrices for

all the steady states and their corresponding eigenvalues. However, I refrain from giving the details for each one of them, the outcome is summarized in the tables below.

| Steady state $(U^*, P^*, W^*) = (0, 0, 1)$ | |
|---|---|
| Eigenvalues | $\lambda_1 = 0 + \dfrac{\delta A}{c}$<br>$\lambda_2 = \sqrt{B} - \delta\dfrac{\tilde{s}}{2}$<br>$\lambda_3 = -\sqrt{B} - \delta\dfrac{\tilde{s}}{2}$ |
| Eigenvectors | $\begin{pmatrix} 0 & \frac{1}{\sqrt{B}} - \frac{\delta\tilde{s}}{2B} & -\frac{1}{\sqrt{B}} - \frac{\delta\tilde{s}}{2B} \\ 0 & 1+\delta & 1+\delta \\ 1+\delta & 0 & 0 \end{pmatrix}$ |

| Steady state $(U_+^*, P_+^*, W_+^*) = (\dfrac{A+\sqrt{A^2-4AB^2}}{2B}, 0, \dfrac{2B^2}{A+\sqrt{A^2-4AB^2}})$ | |
|---|---|
| Eigenvalues | $\lambda_1 = 0 + \dfrac{\delta(A-U_+^*)}{c}$<br>$\lambda_2 = i\sqrt{B} + \delta(\dfrac{U_+^{*2}}{c} - \dfrac{\tilde{s}}{2})$<br>$\lambda_3 = -i\sqrt{B} + \delta(\dfrac{U_+^{*2}}{c} - \dfrac{\tilde{s}}{2})$ |
| Eigenvectors | $\begin{pmatrix} -\frac{U_+^{*2}}{B}(1+\delta) & -\frac{i}{\sqrt{B}} + \delta(-\frac{i}{\sqrt{B}} + \frac{U_+^{*2}}{c} - \frac{\tilde{s}}{2}) & \frac{i}{\sqrt{B}} + \delta(\frac{i}{\sqrt{B}} + \frac{U_+^{*2}}{c} - \frac{\tilde{s}}{2}) \\ \frac{-\delta U_+^{*2}(A-U_+^*)}{cB} & 1+\delta & 1+\delta \\ 1+\delta & -\frac{2\delta}{c} & -\frac{2\delta}{c} \end{pmatrix}$ |

| Steady state $(U_-^*, P_-^*, W_-^*) = (\frac{A-\sqrt{A^2-4AB^2}}{2B}, 0, \frac{2B^2}{A-\sqrt{A^2-4AB^2}})$ | |
|---|---|
| Eigenvalues | $\lambda_1 = 0 + \frac{\delta(A-U_-^*)}{c}$<br>$\lambda_2 = i\sqrt{B} + \delta(\frac{U_-^{*2}}{c} - \frac{\tilde{s}}{2})$<br>$\lambda_3 = -i\sqrt{B} + \delta(\frac{U_-^{*2}}{c} - \frac{\tilde{s}}{2})$ |
| Eigenvectors | $\begin{pmatrix} -\frac{U_-^{*\,2}}{B}(1+\delta) & -\frac{i}{\sqrt{B}} + \delta(-\frac{i}{\sqrt{B}} + \frac{U_-^{*\,2}}{c} - \frac{\tilde{s}}{2}) & \frac{i}{\sqrt{B}} + \delta(\frac{i}{\sqrt{B}} + \frac{U_-^{*\,2}}{c} - \frac{\tilde{s}}{2}) \\ \frac{-\delta U_-^{*\,2}(A-U_-^*)}{cB} & 1+\delta & 1+\delta \\ 1+\delta & -\frac{2\delta}{c} & -\frac{2\delta}{c} \end{pmatrix}$ |

Step 3: In this step we will find the inverse of the eigenvector matrix of the steady state $(U_+^*, P_+^*, W_+^*)$. Since, the eigenvector matrix has elements which are order of $\delta$ we need to split it again and find the inverse of each matrix separately, below is the final result.

$$\begin{pmatrix} 0 & 0 & 1 \\ \frac{i\sqrt{B}}{2} & \frac{1}{2} & \frac{iU_+^{*2}}{2\sqrt{B}} \\ -\frac{i\sqrt{B}}{2} & \frac{1}{2} & -\frac{iU_+^{*2}}{2\sqrt{B}} \end{pmatrix}$$

$$+\frac{\delta}{det}\begin{pmatrix} 0 & -\frac{4i}{c\sqrt{B}} & -\frac{2i}{\sqrt{B}} \\ \frac{c^2B-2U_+^{*2}(A-U_+^*)}{c^2B} & \frac{2U_+^{*2}}{cB} - \frac{i}{\sqrt{B}} - \frac{U_+^{*2}}{c} + \frac{\tilde{s}}{2} & \frac{U_+^{*2}}{B} - \frac{U_+^{*2}(A-U_+^*)}{cB}(\frac{i}{\sqrt{B}} + \frac{U_+^{*2}}{c} - \frac{\tilde{s}}{2}) \\ \frac{2U_+^{*2}(A-U_+^*)-c^2B}{c^2B} & -(\frac{2U_+^{*2}}{cB} + \frac{i}{\sqrt{B}} - \frac{U_+^{*2}}{c} + \frac{\tilde{s}}{2}) & -\frac{U_+^{*2}}{B} + \frac{U_+^{*2}(A-U_+^*)}{cB}(-\frac{i}{\sqrt{B}} + \frac{U_+^{*2}}{c} - \frac{\tilde{s}}{2}) \end{pmatrix}$$

where $det = \frac{4iU_+^{*2}(A-U_+^*) - 2ic^2B}{c^2B^{3/2}}$.

The inverse of the eigenvector matrix is very convoluted, hence the whole transformation will be even more complicated, especially for the translated coordinates. For that reason, I will not show the linear algebra, I will only go through the steps that need to be followed to find the stability of periodic

orbits.

Step 4: Let the system (5.31) be written as $\dot{\tilde{\mathbf{U}}} = J\tilde{\mathbf{U}} + \mathbf{f}(\tilde{\mathbf{U}})$, and the eigenvector matrix corresponding to the steady state $(\tilde{U}^*, \tilde{P}^*, \tilde{W}^*)$, $\mathbf{P}$. We note that $\mathbf{P}$ typically will still have complex entries.
We introduce a new set of coordinates, $\mathbf{x} = (x, y, z)^T$, and we use the basis of the eigenvector matrix $\mathbf{P}$ for the new coordinate system:

$$\tilde{\mathbf{U}} = \mathbf{P} \cdot \mathbf{x} \tag{5.32}$$

The reason we needed to find the inverse matrix of $\mathbf{P}$ in Step 3, is the rearrangment of system (5.32): $\mathbf{x} = \mathbf{P^{-1}} \cdot \mathbf{U}$. So under this transformation, we get the new system:

$$\dot{\mathbf{x}} = \mathbf{P^{-1}}\dot{\tilde{\mathbf{U}}} \tag{5.33}$$

where $\dot{\tilde{\mathbf{U}}} = J\tilde{\mathbf{U}} + \mathbf{f}(\tilde{\mathbf{U}})$.Then

$$\dot{\mathbf{x}} = \mathbf{P^{-1}}(\mathbf{J}\tilde{\mathbf{U}} + \mathbf{f}(\tilde{\mathbf{U}})) \tag{5.34}$$

Since we only need to have coordinates of $\mathbf{x} = (x, y, z)^T$, we replace $\tilde{\mathbf{U}} = \mathbf{P} \cdot \mathbf{x}$. The final form of the transformed system is:

$$\dot{\mathbf{x}} = \mathbf{P^{-1}JP} \cdot \mathbf{x} + \mathbf{P^{-1}f}(\mathbf{P} \cdot \mathbf{x}) \tag{5.35}$$

Then the system will have only $x, y$ and $z$ terms with a linear and nonlinear part:

$$\dot{\mathbf{x}} = \mathbf{A} \cdot \mathbf{x} + \mathbf{g}(\mathbf{x}) \tag{5.36}$$

where $A = \begin{pmatrix} C & 0 & 0 \\ 0 & S & 0 \\ 0 & 0 & U \end{pmatrix}$ and $\dim(x)$=$\dim(E^c)$, $\dim(y)$=$\dim(E^s)$, $\dim(z)$=$\dim(E^u)$.
In terms of the three subsets of variables, the ODEs now take the form

$$\begin{aligned} \dot{x} &= Cx + F(x, y, z) \\ \dot{y} &= Sy + G(x, y, z) \\ \dot{z} &= Uz + H(x, y, z) \end{aligned} \tag{5.37}$$

Step 5: We now look for solutions that are tangent to the center space so that $W^c = \{h(y,z), y, z\}$ [10]. Assume that $x = h(y,z)$ and its power series expansion is $h(y,z) = ay^2 + byz + cz^2 + ...$ Requiring that $x = h(y,z)$ is an invariant manifold, differentiating it will be $\dot{x} = 2ay\dot{y} + by\dot{z} + 2cz\dot{z} + ...$, where $\dot{y}$ and $\dot{z}$ are substituted with the equations from the system (5.37), and if there is an x we substitute it with $ay^2 + byz + cz^2$.
Collecting the nonlinear terms $y^2, z^2, yz$ can give equations with the unknown a,b,c which can be solved and then be determined. Next, we replace the known coefficients a,b and c back to $x = h(y,z) = ay^2 + byz + cz^2$ and substitute it into the original equations of $(y,z)$ of (5.37) which will give the dynamics on the center manifold:

$$\begin{pmatrix} \dot{y} \\ \dot{z} \end{pmatrix} = \begin{pmatrix} S & 0 \\ 0 & U \end{pmatrix} \begin{pmatrix} y \\ z \end{pmatrix} + \begin{pmatrix} G_1(y,z) \\ H_1(y,z) \end{pmatrix} \tag{5.38}$$

where $G_1(y,z)$ and $H_1(y,z)$ are the functions of nonlinear terms and $S$ and $U$ are still complex since we are interested in the Hopf bifurcation.

Step 6: Now we can finally determine the stability of periodic orbits. Since we brought the system (1.6) into a 2D system according to the Hopf Theorem and Center Manifold Theorem, we can now apply the Hopf Bifurcation Theorem mentioned in the Intermezzo section. We introduce the real variables $y, z$, by $y = y + iz$ and $z = y - iz$ and determine the real 2-dimensional system:

$$\begin{pmatrix} \dot{y} \\ \dot{z} \end{pmatrix} = \zeta \begin{pmatrix} y \\ z \end{pmatrix} + \begin{pmatrix} f(y,z) \\ g(y,z) \end{pmatrix} \tag{5.39}$$

where we know that $\zeta = \begin{pmatrix} 0 & -\omega \\ \omega & 0 \end{pmatrix}$ at the Hopf bifurcation. The nonlinear parts $f(y,z)$ and $g(y,z)$ are very important since they are needed for the formula:

$a = \frac{1}{16}(f_{yyy} + g_{yyz} + f_{yzz} + g_{zzz}) + \frac{1}{16\omega}[f_{yz}(f_{yy} + f_{zz}) - g_{yz}(g_{yy} - g_{zz})$
$-f_{yy}g_{yy} + f_{zz}g_{zz}]$.

Assuming from the steps 1-6, that all the four conditions of the Hopf Bifurcation Theorem hold, then:

A) If $a\alpha'(0) < 0$, a unique limit cycle bifurcates from the origin in $\mu > 0$ as $\mu$ passes through 0. The stability of the limit cycle [in $\mu > 0$] is the same as the stability of the origin in $\mu < 0$.

B) If $a\alpha'(0) > 0$, a unique limit cycle bifurcates from the origin in $\mu < 0$ as $\mu$ passes through 0. The stability of the limit cycle [in $\mu < 0$] is the same as the stability of the origin in $\mu > 0$.

# Conclusion

One of the main objectives of this thesis was to prove the existence of homoclinic and periodic orbits. Using the information stated in the Introduction that periodic patterns travel towards an uphill direction, we started the analysis of the model (2) by applying the geometric singular perturbation theory in Chapter 2. After proving successfully the existence of homoclinic and periodic orbits the next challenging aim was to find their stability.

Even though, all the mathematical analysis of this thesis concerns the ODE system (1.6), the constructed solutions are still related to the original model, which is a PDE system (2). For instance, it is known that if the critical point of the (planar) ODE system associated to a scalar reaction-diffusion equation is saddle, respectively a center point, then the trivial solution of the original PDE system would be stable, respectively unstable, and vice versa. Similarly, although more invaded, statements hold for relation between the local character of critical points of ODE reductions of 2- component react-diffusion PDEs, see [3].

The mathematical expression of a periodic orbit as shown in chapter five, is formed by the equation $y = r\cos(\omega t + \phi)$, which describes an oscillation where $r$ is the amplitute, $\phi$ is the phase and $\omega$ is its angular velocity. Some patterns mentioned in the Introduction correspond to such periodic solutions. Therefore by finding the stability of the periodic orbits of the system (1.6) it would provide by analogy to the above mentioned example of critical points a very relevant insight, into ecological implications such as the patterns which can be observed.

We chose to focus on the stability of periodic orbits which are very close to

the Hopf Bifurcation point. This approach would be more feasible to be studied instead of focusing on the periodic orbits near the homoclinic bifurcation, the stability can in principle be determined near the homoclinic limit, but the technicalities are even more involved than in the Hopf bifurcation case.
Due to natural time restrictions and the overwhelming technicalities regarding the linear algebra and center manifold analysis, as mentioned in fifth chapter, we have decided to focus on the underlying mechanisms without explicitly deriving a final result on the stability of periodic orbits.

Nowadays the technology is rapidly evolving and a lot of mathematical models of real life phenomena are implemented into computational software while the explicit analysis of these models is largely neglected. Nonetheless, in order to be able to create algorithms and implement such problems into the computational field, besides the mathematical model explicit analytical insights are needed, which come from the mathematical analysis on a theoretical level. Also, regarding these kind of systems, usually there are many parameters that cannot be dealt with numerical simulations or numerical analysis, so the combination with explicit analysis is mandatory.

Besides all the limitations that appeared during the completion of the thesis, there is ample motivation for further research. By following the steps in section 5.2, the PDE system (2) can be transformed into a system of equations in the form of (5.39). It will be natural to also implement it into software and study the pattern formation with actual parameter values. Moreover, finding the stability of periodic orbits as another research topic may be a small part of a bigger project on trying to predict vegetation dynamics under future circumstances. It seems quite ambitious but analyzing a system explicitly and on a theoretical level provides a comprehensive understanding of a model.

In addition to the insights provided in the ecological implications by the mathematical procedure, this thesis could also be used as a helpful handout to students who are interested in dynamical systems and perturbation theory. There are many methods related to these specific areas, where students can actually

study theorems applied in a real life model but also use it as a supplementary paper for some mathematical methodologies.

# Bibliography


[1] A. Doelman. Traveling waves in the complex Ginzburg-Landau equation. *Journal of Nonlinear Science*, 3(1):225–266, Dec 1993.

[2] Arjen Doelman. Slow time-periodic solutions of the Ginzburg-Landau equation. *Physica D: Nonlinear Phenomena*, 40(2):156 – 172, 1989.

[3] Arjen Doelman. *Pattern formation in reaction-diffusion systems an explicit approach*, pages 129–182. 04 2019.

[4] Arjen Doelman and Philip Holmes. Homoclinic explosions and implosions. *Philosophical Transactions: Mathematical, Physical and Engineering Sciences*, 354(1709):845–893, 1996.

[5] Geertje Hek. Geometric singular perturbation theory in biological practice. *Journal of Mathematical Biology*, 60(3):347–386, Mar 2010.

[6] Mark H Holmes. *Introduction to Perturbation Methods*. Texts in applied mathematics ; 20. Springer, New York, 2nd ed.. edition, 2013.

[7] Ferdinand Verhulst Jan A. Sanders and James Murdock. Averaging methods in nonlinear dynamical systems. *SIAM Review*, 29(1):157–158, 1987.

[8] Christopher A. Klausmeier. Regular and irregular patterns in semiarid vegetation. *Science*, 284(5421):1826–1828, 1999.

[9] J. E Marsden and M Mccracken. *The Hopf Bifurcation and Its Applications*, volume 19 of *Applied Mathematical Sciences,*. Springer New York, New York, NY, 1976.

[10] J. Meiss. *Differential Dynamical Systems*. Society for Industrial and Applied Mathematics, 2007.

[11] Francisco Armando Carrillo Navarro and Fernando Verduzco Gonzalez. Control of the Hopf bifurcation in the Takens-Bogdanov bifurcation. *2008 47th IEEE Conference on Decision and Control*, pages 4438–4443, 2008.

[12] Mattia Sensi. Homoclinic vegetation stripes in a Klausmeier- Gray- Scott model, 2017.

[13] Jonathan A Sherratt. Pattern solutions of the Klausmeier model for banded vegetation in semi-arid environments i. *Nonlinearity*, 23(10):2657, 2010.

[14] E. Siero, A. Doelman, M. B. Eppinga, J. D. M. Rademacher, M. Rietkerk, and K. Siteur. Striped pattern selection by advective reaction-diffusion systems: Resilience of banded vegetation on slopes. *Chaos: An Interdisciplinary Journal of Nonlinear Science*, 25(3):036411, 2015.

[15] Ferdinand Verhulst. *Nonlinear Differential Equations and Dynamical Systems*. Springer-Verlag, Berlin, Heidelberg, 1990.